

Review

State of Art and Perspectives in Catalytic Ozonation for Removal of Organic Pollutants in Water: Influence of Process and Operational Parameters

Naghmeh Fallah ^{1,*} , Ermelinda Bloise ¹ , Domenico Santoro ² and Giuseppe Mele ¹ ¹ Department of Engineering for Innovation, University of Salento, Via Monteroni, 73100 Lecce, Italy² Department of Chemical and Biochemical Engineering, University of Western Ontario, London, ON N6A 5B9, Canada

* Correspondence: naghmeh.fallah@unisalento.it

Abstract: The number of organic pollutants detected in water and wastewater is continuously increasing thus causing additional concerns about their impact on public and environmental health. Therefore, catalytic processes have gained interest as they can produce radicals able to degrade recalcitrant micropollutants. Specifically, catalytic ozonation has received considerable attention due to its ability to achieve advanced treatment performances at reduced ozone doses. This study surveys and summarizes the application of catalytic ozonation in water and wastewater treatment, paying attention to both homogeneous and heterogeneous catalysts. This review integrates bibliometric analysis using VOS viewer with systematic paper reviews, to obtain detailed summary tables where process and operational parameters relevant to catalytic ozonation are reported. New insights emerging from heterogeneous and homogenous catalytic ozonation applied to water and wastewater treatment for the removal of organic pollutants in water have emerged and are discussed in this paper. Finally, the activities of a variety of heterogeneous catalysts have been assessed using their chemical-physical parameters such as point of zero charge (PZC), pKa, and pH, which can determine the effect of the catalysts (positive or negative) on catalytic ozonation processes.

Keywords: catalytic ozonation; homogenous catalysts; heterogeneous catalysts; water treatment; VOSviewer; reaction mechanism



Citation: Fallah, N.; Bloise, E.; Santoro, D.; Mele, G. State of Art and Perspectives in Catalytic Ozonation for Removal of Organic Pollutants in Water: Influence of Process and Operational Parameters. *Catalysts* **2023**, *13*, 324. <https://doi.org/10.3390/catal13020324>

Academic Editors: Gassan Hodaifa, Rafael Borja and Mha Albqmi

Received: 23 December 2022

Revised: 24 January 2023

Accepted: 28 January 2023

Published: 1 February 2023



Copyright: © 2023 by the authors. Licensee MDPI, Basel, Switzerland. This article is an open access article distributed under the terms and conditions of the Creative Commons Attribution (CC BY) license (<https://creativecommons.org/licenses/by/4.0/>).

1. Introduction

Industrial wastewater has been under extensive research due to its hazardous effect on the aquatic, air, and soil environment, as well as human and animal health. Developing wastewater treatment technologies that are simple, safe, and efficient for the environment is becoming the twenty-first century's primary goal.

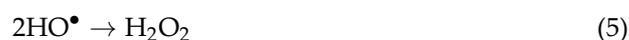
Advanced oxidation processes (AOPs) have shown great potential for the degradation and mineralization of recalcitrant and toxic organic pollutants compared to conventional treatment processes. This process is classified into two main general categories. The first category utilizes light energy such as ultraviolet (UV) light in conjunction with other chemical additives. There are processes under this category that associate other agents with UV, such as hydrogen peroxide (UV/H₂O₂), ozone (UV/O₃), titanium oxide (UV/TiO₂), and Fenton reagents (UV/Fenton). When no light source is used, the technology can be termed a dark oxidative process. Processes in this category include ozonation, Fenton's reagent, ultrasound, and microwaves. These processes are simultaneously based on the in situ generations of highly reactive transitory species (H₂O₂, HO•, O²⁻, O₃) for the mineralization of refractory organic compounds and the inactivation of waterborne pathogens. Due to rapid oxidation reactions, AOPs are characterized by high reaction rates and short treatment times, which make them promising in wastewater treatment [1].

Ozone is a powerful oxidant with several advantages that make it an excellent material in the AOPs. There are many noticeable benefits of using O₃ in the wastewater treatment process. Benefits such as it rapidly reacting with bacteria, viruses, and protozoa, being efficient for organics degradation and inorganics removal, and removing color, taste, and odor. Although the ozonation process is a practical system, O₃ has low solubility and stability in water and a high production cost. To solve the mentioned disadvantages, some solutions have been explored, such as using fixed beds of porous glass or metals, solid catalysts, stirring, line mixers, contact towers, and an increase in retention time by large bubble columns or diffusers [1]. The combination of ozonation with other techniques is suggested as an intelligent solution. In this regard, various O₃-based AOPs, such as OH⁻/O₃, O₃/H₂O₂, O₃/UV, O₃/H₂O₂/UV, O₃/S₂O₈²⁻, O₃/biological treatment, and catalytic and photocatalytic ozonation, were introduced to the industry [2–7]. Each of these processes has its specific features and conditions.

In the OH⁻/O₃ process, the pH value of the water matrices has a significant influence on both the direct ozonation efficiency and the generation of HO• (indirect ozonation). At significantly high pH (pH > 8), the abundance of OH⁻ can improve HO• generation, which will enhance the ozonation of pollutants. However, high pH might cause the precipitation of calcium carbonate or other problems, which should be considered. In addition, the pH adjustment will increase the operational cost. In the so-called peroxone technique, O₃ and H₂O₂ would be combined [8]. The critical effect of combining O₃ and H₂O₂ is increasing oxidation efficiency. This occurs by converting O₃ to HO• and improving O₃ transfer from the gas to the liquid phase [8]. The chemistry of the main reactions described above is shown in Equations (1)–(3).



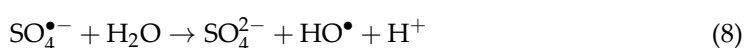
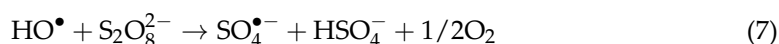
Another ozonation technique is the usage of ultraviolet light in combination with O₃ in an aqueous medium. This combination causes the increase in the HO• formation and its concentration, consequently increasing the degradation efficiency. Equations (4) and (5) show that the formation of H₂O₂ as a by-product is possible, which will be degraded by the exact mechanism of H₂O₂/UV [8], also increasing the treatment efficiency.



The introduction of UV with H₂O₂/O₃ makes the previously mentioned techniques more efficient. This combination enhances HO• generation and more efficiently allows the transformation of H₂O₂ to HO• (Equation (6)) [9], consequently increasing the degradation rate.



Persulfate S₂O₈²⁻ as a practicable material for water treatment would be combined with O₃. It is assumed that O₃ decomposes with the formation of HO•, which can then activate persulfate to generate SO₄^{•-} (Equation (7)) [10]. In turn, SO₄^{•-} can increase the formation of HO•, which leads to a multiradical system (Equations (8) and (9))



A popular ozonation process is an ozonation/biological treatment technology. This process can be divided into two types: (1) ozonation is used as pre-treatment, such as an O_3 -biological activated carbon process, ozonation/batch aerobic biological system, and ozonation/aerated biological filter; (2) ozonation is used as post-treatment, such as membrane bioreactor/ozonation, activated-sludge biological treatment/ozonation, and sequencing batch biofilm reactor/ozonation. Since the intermediate products formed by ozonation and O_3 -based processes are generally more biodegradable than their precursors, these intermediates can be much more easily removed by biological treatment processes. Therefore, if the water containing many inhibiting compounds is toxic to the biological cultures, in such cases, a biological treatment followed by pre-treatment ozonation is suitable for the application. On the other hand, if there are many biodegradable compounds, the pre-oxidation step obviously will only lead to the unnecessary consumption of chemicals. In this case, a biological pre-treatment followed by ozonation (removing non-biodegradable and toxic components with less oxidant consumption) may be more suitable [11].

In the ozonation process, the addition of some catalysts can promote the decomposition of the oxidant (O_3) to generate active free radicals, such as HO^\bullet . Compared with other O_3 -based treatment methods, catalytic ozonation can reduce operational costs since it does not need additional energy costs such as for UV or for pH adjustment due to its effectiveness in a wide range of pH values. Moreover, the catalytic ozonation systems have shown exemplary performance in water treatment, with several advantages compared to ozonation alone. Several pieces of evidence based on published articles show that the catalytic ozonation process achieved higher mineralization of various organic compounds than the sole ozonation system [12]. All of these reasons make catalytic ozonation an interesting water treatment process and one of the main AOPs processes that received significant attention from scientists. Figure 1 shows the gradual increase in scientific publication since 2000 based on approximately 600 published articles found in the Web of Science collection database.

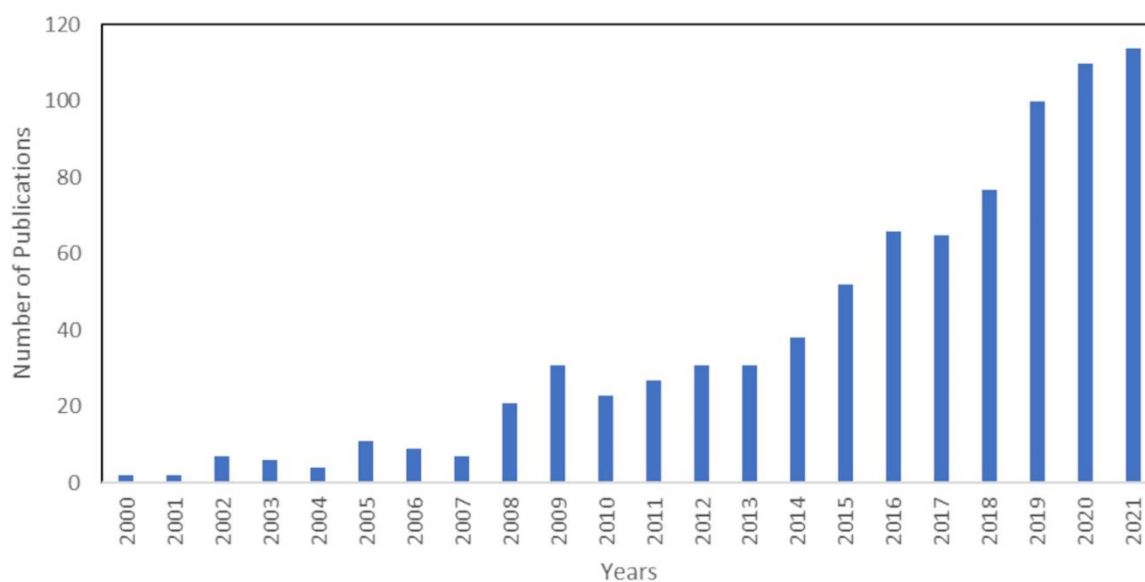


Figure 1. Published articles related to catalytic ozonation since 2000.

During these years, several catalysts have been proven to be effective in the enhancement of ozonation efficiency. Generally, the catalytic ozonation process can be divided into two types:

- (1) Homogeneous catalytic ozonation, in which transition metal ions used as catalysts influence the rate of reaction, the selectivity of O_3 oxidation, and the efficiency of O_3 utilization. Two major mechanisms of homogeneous catalytic ozonation can be found: the O_3 decomposition by metal ions which generates free radicals; and the

complex formation between the metal ions and organic molecule following oxidation of the complex.

- (2) Heterogeneous catalytic ozonation, which is based on the activation of O_3 to improve the ozonation of pollutants in the presence of a solid catalyst. Obviously, the key point in this process is to find the most appropriate catalyst, which is a solid material that in combination with O_3 shows a greater removal of a pollutant at a given pH value, compared to the separate processes of adsorption or ozonation alone. Among the most widely used catalysts in heterogeneous catalytic ozonation are metal/bimetal/polymetal oxides, metal/metal oxides on supports, carbon-based materials, and the emerging category of multifunctional porous materials as metal–organic frameworks. The role of the catalyst in this process is to provide reaction sites for adsorption and catalysis. So, based on the interaction of catalysts with O_3 and micropollutants, three general major mechanisms can be found. (a) Adsorption of O_3 on the catalyst surface following O_3 decomposition to generate free radicals; (b) adsorption of micropollutants on the catalyst surface, then attacking by O_3 molecule; (c) adsorption of both O_3 and micropollutants on the catalyst and their reaction together.

Many factors may have an impact on the performance of the catalysts. The PZC value of the material, the acid/basic sites of the surface, the oxidative potential of the metals contained in the solid structure, the cation exchange capacity, the oxygen vacancies, etc., are examples of these factors [13–15]. An important research aspect is the specific role played by the point of zero charge (PZC) in the overall efficiency of the catalytic ozonation process. Several researchers measured the PZC value of their synthesized catalyst and explained their surface characteristics based on this factor [16–21]. On the other hand, there are studies that examined the role of oxygen vacancies in catalytic ozonation [14,22], and the effect of the lewis acid/basic sites of the surface [23–27]. Although there are some studies that prove that these two factors can also influence O_3 decomposition, there are a variety of papers in which authors do not report, nor discuss, the impact of these factors.

In the terms of process efficiency of catalytic ozonation, operational parameters and reaction mechanism in the process have a big impact. According to operational parameters, initial solution pH, O_3 dose, initial pollutant concentration, pressure, catalyst dosage, and temperature have major effects on efficiency. Our attention has been placed on the governing mechanisms of the process based on the chemical properties of catalysts, physical properties of catalysts, natural properties of target pollutants (pKa), and pH of the solution as described in this article.

2. A Bibliometric Analysis Using VOSviewer

The scientific articles about catalytic ozonation published between 2000 and 2021 were scanned in the Web of Science (WOS) collection database. The words “Catalytic Ozonation” were used as the keywords to achieve the relevant publications. VOS viewer was applied to perform the bibliometric analysis of these articles. In this respect, 600 publications on the topic of catalytic ozonation were identified in the WOS core database.

Bibliometric analysis of the keywords in publications was studied. In this respect, all provided keywords in the articles related to catalytic ozonation that occurred more than 20 times in the WOS core database were enrolled in the final analysis. Based on the catalytic ozonation articles in the English language, of the 1441 keywords accrued, 26 of these keywords had appeared 20 times more frequently than the others. The keyword “catalytic ozonation” was the most frequently occurring one, with an occurrence of 197 and total link strength of 177. Following the previously mentioned keyword, “ozone”, “degradation”, and “oxidation” occurred 169, 154, and 129 times, respectively. Figure 2 illustrated the bibliometric analysis and VOSviewer visualization of the keywords in articles related to catalytic ozonation.

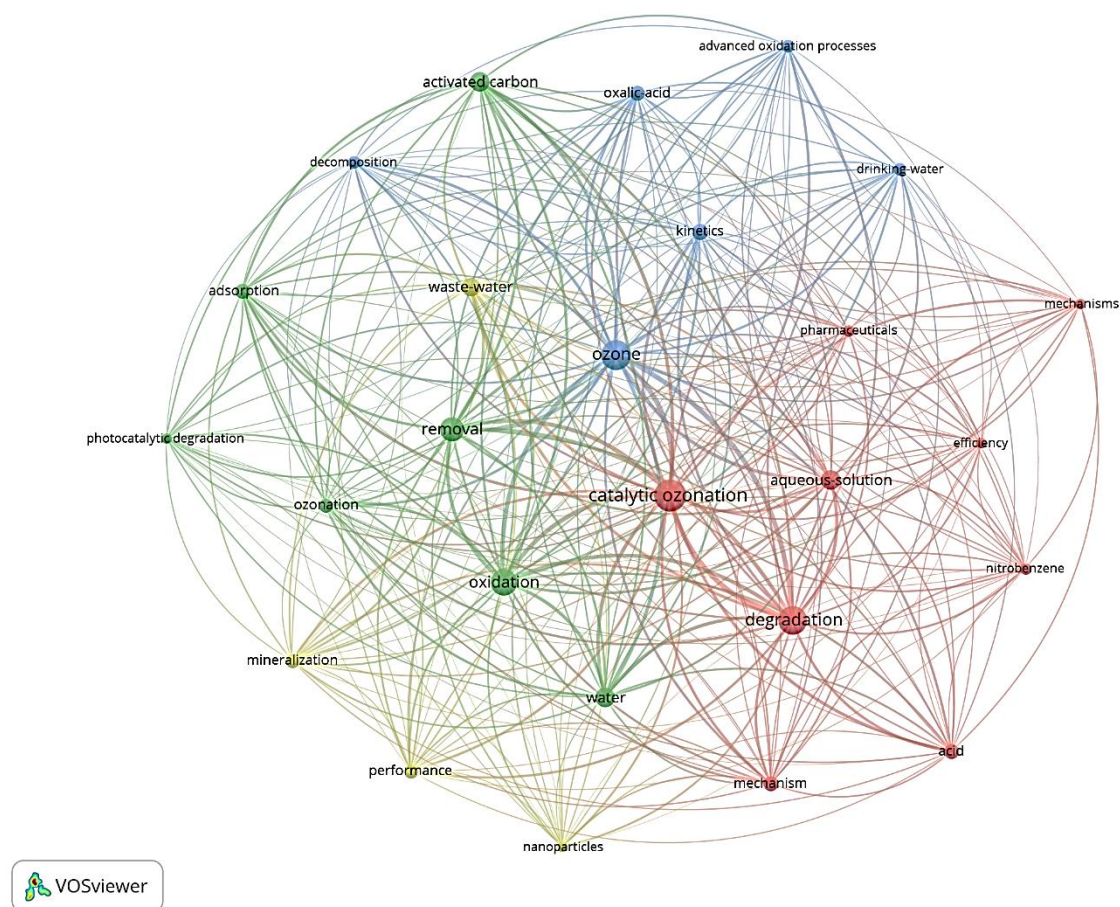


Figure 2. Co-occurrence of the keywords in articles related to catalytic ozonation visualized by VOSviewer software.

Based on the WOS collection database results in the case of ‘catalytic ozonation’, a bibliometric analysis of the co-authorship between countries was studied. All countries that published more than five articles in the WOS core database related to catalytic ozonation were enrolled in the final analysis.

In this respect, the top ten most active countries in the field of catalytic ozonation based on the number of citations, publications, and total link strength, are listed in Table 1. Of the 47 countries that worked on catalytic ozonation topics, 14 countries had more than 5 published articles. Based on the information gathered, the country most active in the field of catalytic ozonation is “China”, with 185 publications, 422 citations, and a total link strength of 20. Following that, Iran and Canada take second and third places, respectively.

All these bibliometric analyses show the importance of catalytic ozonation among scientists all around the world. In the absence of a comprehensive and precise survey about the developments in catalytic ozonation processes, it would not be easy to propose novel investigations to optimize water treatment performance in terms of mineralization, industrial application, and economic capability. In light of these considerations, this study aims to recognize the popular and leading articles in catalytic ozonation, summarizing new visions on the evaluation of both heterogeneous and homogeneous processes for the degradation and mineralization of various toxic organic pollutants in water.

Table 1. The top 10 active countries in the field of catalytic ozonation.

Rank	Country	Number of Citations	Number of Documents	Total Link Strength
1	China	422	185	20
2	Iran	82	37	4
3	Canada	38	14	5
4	USA	41	13	8
5	Pakistan	28	12	8
6	Brazil	22	8	1
7	Turkey	25	8	1
8	France	23	8	0
9	Australia	10	7	5
10	Greece	14	7	1

3. Homogeneous Catalytic Ozonation

Transition metals such as Fe(II), Fe(III), Mn(II), Ni(II), Co(II), Pb(II), and Zn(II) used as homogenous catalysts in the aqueous solution are commonly involved in two mechanistic steps of the ozonation processes: initiation of the O₃ decomposition reaction followed by the generation of the hydroxyl radicals, and oxidation reaction between catalyst and organic pollutants. Some homogeneous catalytic systems selected among the most influencing articles reported in the current literature are listed in Table 2. Details regarding the kind of used catalysts, target pollutants, operating conditions, and removal results are included in this table.

Table 2. Literature reports on different homogenous catalysts in the ozonation process.

Target Pollutants	Catalysts	Operating Conditions	Removal Results	Ref.
Aniline	Fe(II)	O ₃ dose: 0.5 g/h; Catalyst dose: 1 mmol/dm ³ ; pH: 3.3; T: 25 °C; t: 15 min	132 TOC removal	[28]
4-chlorophenol	Fe(II)	O ₃ dose: 0.5 g/h; Catalyst dose: 1 mmol/dm ³ ; pH: 3.3; T: 25 °C; t: 15 min	144 TOC removal	[28]
Oxalic acid (OA)	Fe(III)	O ₃ dose: 8.2 mg/L; Catalyst dose: 1 mg/L; pH: 2; T: 20 °C; t: 3 h	7% OA removal	[29]
1,3,6-naphthalenetrisulfonic acid (NTS)	Fe(II)	O ₃ dose: 1.04 × 10 ⁻⁴ mol/dm ⁻³ ; Catalyst dose: 1.25 × 10 ⁻⁴ mol/dm ⁻³ ; pH: 2; T: 25 °C; t: 30 min	79% NTS degradation	[30]
Lipid	Fe(II)	O ₃ dose: 0.6 g/L; Catalyst dose: 7 mg/L; pH: 6.75; T: 25 °C; t: 60 min	96.7% lipid degradation	[31]
Chlorobenzenes	Fe(II)	O ₃ dose: 1.5 g O ₃ /TOC; Catalyst dose: 6 × 10 ⁻⁵ mol/L; pH: 7; t: 20 min	55% COD removal	[32]
Chlorobenzenes	Fe(III)	O ₃ dose: 1.5 g O ₃ /TOC; Catalyst dose: 6 × 10 ⁻⁵ mol/L; pH: 7; t: 20 min	12% COD removal	[32]
Aniline aerofloat (AAF)	Fe(II)	O ₃ dose: 2.08 mg/min. L; Catalyst dose: 10 mg/L; pH: 8; T: 25 °C; t: 180 min	80% COD removal	[33]
AAF	Fe(III)	O ₃ dose: 2.08 mg/min. L; Catalyst dose: 10 mg/L; pH: 8; T: 25 °C; t: 180 min	76% COD removal	[33]
C.I. Reactive Red 2 (RR2)	Fe(III)	O ₃ dose: 200 mL/min; Catalyst dose: 0.6 mM; pH: 2; T:NR; t: 6 min	1.278 of decolorization rates (1/min)	[34]
RR2	Fe(II)	O ₃ dose: 200 mL/min; Catalyst dose: 0.6 mM; pH: 2; T:NR; t: 6 min	1.299 of decolorization rates (1/min)	[34]
p-Chlorobenzoic acid (p-CBA)	Fe(II)	O ₃ dose: 2 mg/L; Catalyst dose: 1 mg/L; pH: 7; T: 23 °C; t: 15 min	92.5% p-CBA degradation	[35]
RR2	Zn(II)	O ₃ dose: 200 mL/min; Catalyst dose: 0.6 mM; pH: 2; T:NR; t: 6 min	1.015 of decolorization rates (1/min)	[34]

Table 2. Cont.

Target Pollutants	Catalysts	Operating Conditions	Removal Results	Ref.
p-CBA	Co(II)	O ₃ dose: 2 mg/L; Catalyst dose: 1 mg/L; pH: 7; T: 23 °C; t: 15 min	95.5% p-CBA degradation	[35]
RR2	Co(II)	O ₃ dose: 200 mL/min; Catalyst dose: 0.6 mM; pH: 2; T:NR; t: 6 min	0.843 of decolorization rates (1/min)	[34]
OA	Co(II)	O ₃ dose: 30 mg/L; Catalyst dose: 0.8 mg/L; pH: 2.5; T:NR; t: 90 min	70% OA removal	[36]
OA	Co(II)	O ₃ dose: 5 × 10 ⁻³ mol/L; Catalyst dose: 4 mg/L; pH: 2.5; T: 25 °C; t: 30 min	99.3% TOC removal	[37]
Formic acid	Co(II)	O ₃ dose: 5 × 10 ⁻³ mol/L; Catalyst dose: 4 mg/L; pH: 2.5; T: 25 °C; t: 35 min	60.2% TOC removal	[37]
Carboxylic acids	Cu(II)	O ₃ dose: 71 mg/L; Catalyst dose: 20 µg/L; pH: natural; T:NR; t:NR	75% TOC reduction	[38]
AAF	Cu(II)	O ₃ dose: 2.08 mg/min. L; Catalyst dose: 10 mg/L; pH: 8; T: 25 °C; t: 180 min	75% COD removal	[33]
N-dimethylpropyl-2-pyrrolidone (NDPP)	Pd(II)	O ₃ dose: 250 mL/min. L; Catalyst dose: 9.4 × 10 ⁻⁵ M; pH: 2; T: 25 °C; t: 30 min	73% NDPP removal	[39]
RR2	Ni(II)	O ₃ dose: 200 mL/min; Catalyst dose: 0.6 mM; pH: 2; T:NR; t: 6 min	0.822 of decolorization rates (1/min)	[34]
RR2	Mn(II)	O ₃ dose: 200 mL/min; Catalyst dose: 0.6 mM; pH: 2; T:NR; t: 6 min	3.295 of decolorization rates (1/min)	[34]
Pyruvic acid	Mn(IV)	O ₃ dose: 0.5 g/h; Catalyst dose: 200 mg; pH: 3; T: 25 °C; t: 60 min		[40]
Atrazine (ATZ)	Mn(II)	O ₃ dose: 2.54 mg/L; Catalyst dose: 0.3 mg/L; pH: 7; T: 21 °C; t: 4 min	96% ATZ removal	[41]
ATZ	Mn(II)	O ₃ dose: 2.28 mg/L; Catalyst dose: 1 mg/L; pH: 7; T: 23 °C; t: 5 min	70% ATZ removal	[42]
ATZ	Mn(IV)	O ₃ dose: 2.28 mg/L; Catalyst dose: 1 mg/L; pH: 7; T: 23 °C; t: 5 min	37% ATZ removal	[42]
2,4-dinitrotoluene (DNT)	Mn(II)	O ₃ dose: 5.6 mg/L; Catalyst dose: 0.2 mg/L Mn ²⁺ and 4 mg/L OA; pH: 5.5; T: 25 °C; t: 15 min	65% DNT removal	[43]
2,4-dichlorophenol	Mn(II)	O ₃ dose: 8.4 mg/L; Catalyst dose: 0.5 mg/L; pH: 5.5; T: 25 °C; t: 30 min	80% TOC removal	[44]
NTS	Mn(II)	O ₃ dose: 1.04 × 10 ⁻⁴ mol/dm ⁻³ ; Catalyst dose: 1.25 × 10 ⁻⁴ mol/dm ⁻³ ; pH: 2; T: 25 °C; t: 30 min	72% NTS degradation rate	[30]
OA	Mn(II)	O ₃ dose: 5 × 10 ⁻³ mol/L; Catalyst dose: 4 mg/L; pH: 2.5; T: 25 °C; t: 30 min	82% TOC removal	[37]
Formic acid	Mn(II)	O ₃ dose: 5 × 10 ⁻³ mol/L; Catalyst dose: 4 mg/L; pH: 2.5; T: 25 °C; t: 35 min	61% TOC removal	[37]
Chlorobenzenes	Mn(II)	O ₃ dose: 1.5 g O ₃ /TOC; Catalyst dose: 6 × 10 ⁻⁵ mol/L; pH: 7; T:NR; t: 20 min	66% COD removal	[32]
Lipid	Mn(II)	O ₃ dose: 0.6 g/L; Catalyst dose: 3 mg/L; pH: 6.75; T: 25 °C; t: 60 min	93% lipid degradation	[31]
Simazine	Mn(II)	O ₃ dose: 9.5 mg/L; Catalyst dose: 0.2 mg/L; pH: 7; T: 25 °C; t: 30 min	90% Simazine conversion	[45]

NR-value not reported, TOC total organic carbon, COD chemical oxygen demand.

Different kinds of transitional metals are used as homogeneous catalysts however, Fe(II) and Mn(II) have been reported to be the most efficient catalysts for water purification purposes. This trend in the research has underlying scientific logic. By focusing on the general features of these transition metals' chemistry, their wide range of oxidation states, and complex ion formation, this popularity for using them as a catalyst makes sense. Mn with an atomic number of 25 has the highest number of unpaired electrons in the d-subshell, and it shows variable oxidation states in its compounds such as (II) in Mn²⁺, (III) in Mn₂O₃, (IV) in MnO₂, (VI) in MnO₄²⁻, and (VII) in MnO₄⁻. Fe has two standard oxidation states, Fe²⁺ and Fe³⁺, and a less common (VI) oxidation state in FeO₄²⁻. Existing unpaired electrons and vacant orbitals in these transition metal structures enable them to accept electrons from other ions of molecules to form complex compounds. So this ability causes the adsorption of other substances onto their surface and activates them in the pro-

cess, which is the objective function of a catalyst. The application of these two important transitional metals is explained in the following publications as examples.

Ramos et al. [31] evaluated the efficiency of the Fe(II) catalyst in the ozonation process for lipid degradation. Milk was chosen as the lipid source. It is observed that under neutral conditions, low catalyst dosages are enough to cause the almost complete degradation of lipids (96.7%). Fu et al. [33] investigated the homogeneous catalytic ozonation of AAF collector by coexisting transition metallic ions (Fe(II), Fe(III), Cu(II), Pb(II), and Zn(II)) in flotation wastewaters. Based on this research, the following order of the degradation rate was achieved: $O_3/Fe(II) > O_3/Fe(III) > O_3/Cu(II) > O_3/Pb(II) > O_3/Zn(II) \approx O_3$ -alone. The best catalytic activity gained by Fe(II) had a 31.15% growth of degradation rate and achieved an increase of 42.26% for the AAF mineralization compared to O_3 -alone. Xiao et al. [44] studied the mineralization of DCP in the ozonation process with Mn(II) as a catalyst. This study suggested that in the optimal condition of 0.5 (mg/L) catalyst dose and pH: 5.5, Mn(II) catalytic ozonation had a strong ability to degrade DCP and had 80% TOC removal in water solution.

In terms of the popularity of using this process, it is worth noting that most of the studies related to homogenous catalytic ozonation belong to the first decade of the 20th century. As can be observed in the table, the most significant disadvantage is that this catalytic process is mainly carried out in acidic pH values and not near the natural pH. At the same time, micropollutants, mostly emergent organic pollutants, usually exist in wastewater at the pH range of 6–8. Noting that although homogeneous catalytic ozonation processes can effectively improve the removal of organic contaminants in water in some cases, the addition of metal ions might result in secondary pollution, which causes limiting of their application.

However, in previous years, some scientists showed interest in using transitional metals for the catalytic ozonation process, working at the natural pH and real wastewater. Furthermore, some scientists solved the drawback of introducing these harmful metal ions in the aqueous environment by presenting the idea that some of these transition metallic ions usually coexisted in real wastewater. Several studies confirmed that Fe^{2+} , Cu^{2+} , Zn^{2+} , Pb^{2+} , and Co^{2+} , usually coexist with flotation reagents in the flotation pulp because of the dissolution of minerals or in the bastnaesite flotation pulp, some transition metal ions such as Fe^{2+} , Cu^{2+} , Zn^{2+} , and Pb^{2+} were determined [46,47]. Finally, Fu and colleagues [33] showed that these coexisting transition metallic ions can be used as in situ catalysts. So, it can be deduced that this process can have pleasing prospects by considering some improvements in the future.

4. Heterogeneous Catalytic Ozonation

Catalysts in solid form with high stability and efficiency were widely studied in catalytic ozonation systems. In this section, the activity and efficiency of heterogeneous catalysts in the ozonation process have been evaluated by focusing our attention on essential parameters such as:

- Chemical properties of catalysts: crystallographic and morphological, chemical stability.
- Physical properties of catalysts: point of zero charge (PZC), mechanical strength, surface area, pore volume, and porosity.
- Natural properties of target pollutants (pKa) and pH of the solution.

In each category of catalysts, these parameters are different to achieve the optimum efficiency in the water treatment process. Previous review articles [1,15,48] mentioned that the mechanism of catalytic ozonation is too complicated due to the contradictory catalytic mechanisms proposed by different research groups. In this article, by scrutinizing the governed mechanism of the process based on their conditions, this lack of understanding would have new interpretations.

Generally, the interaction between catalyst, pollutant, and O_3 determines the governing mechanism of this process. Moreover, each of these active components' behaviors depends on other factors and some of these have more influence than others. In the follow-

ing, possible conditions based on the most influencing factors for each active component are expressed, and the governing mechanism in each specific condition is discussed.

Considering that the PZC is generally described as the pH value at which the net charge of the catalyst’s surface is equal to zero.

The positively charged surface catalyst could be found under three different conditions which are proposed in Figure 3.

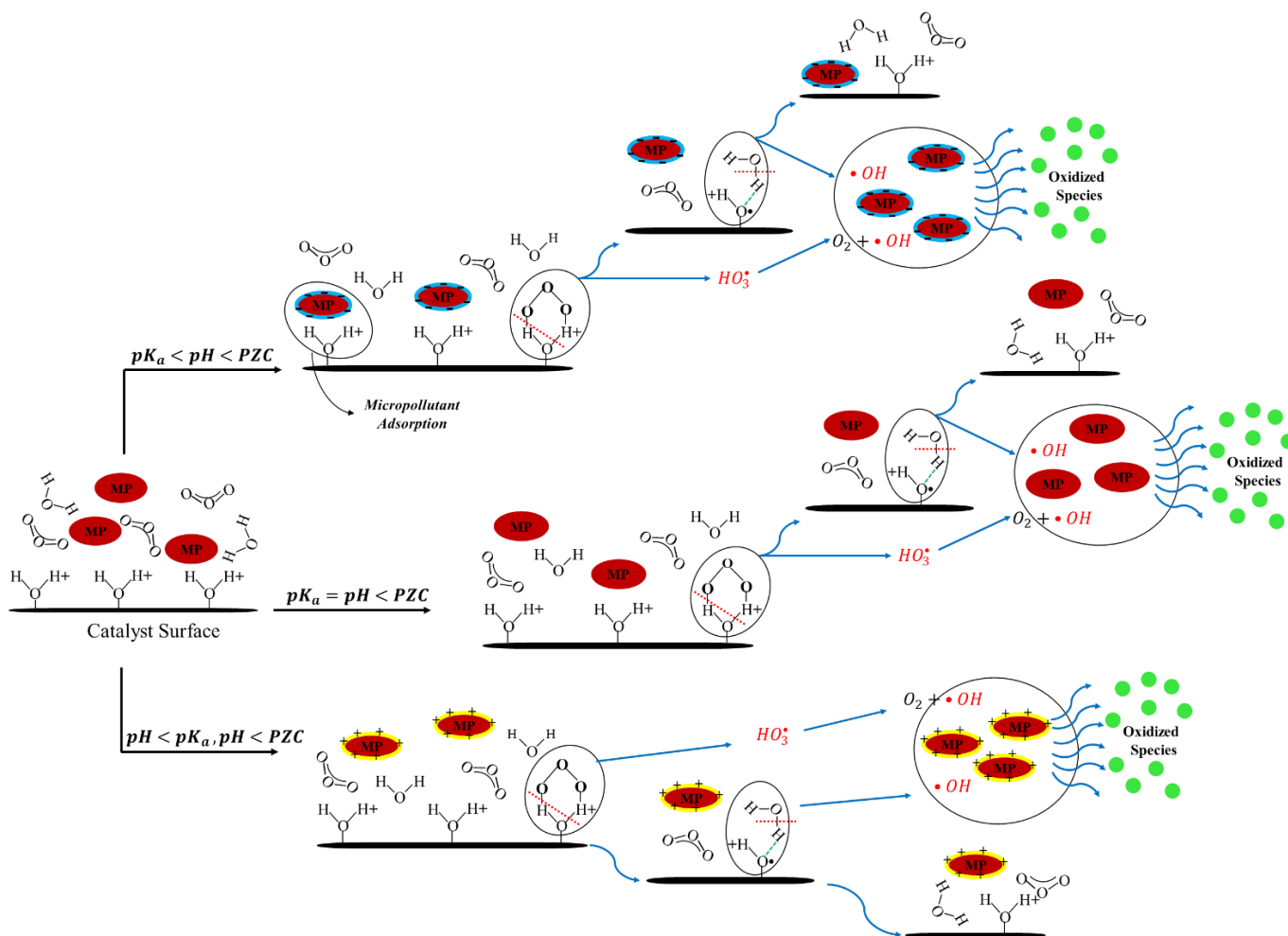


Figure 3. Proposed three influencing mechanisms using positively charged catalysts.

$pK_a < pH < PZC$: Catalyst is positively charged, pollutant is negatively charged.

In this condition, the negatively charged micropollutants can be adsorbed on the positively charged catalyst surface. Thus, the contaminants would be close to the area where the generation of HO^{\cdot} radicals happens, which means HO^{\cdot} can quickly oxidize them in the environment. On the other hand, by adsorbing the micropollutants on the catalyst surface, the active area for adsorption of O_3 will be limited, which has a negative effect on the HO^{\cdot} generation in the environment.

$pH < PZC, pH = pK_a$: Catalyst is positively charged, pollutant is uncharged.

There is no effective interaction between the catalyst and micropollutant in this condition, so the generation of HO^{\cdot} by O_3 decomposition is the only effective parameter here.

$pH < PZC, pH < pK_a$: Catalyst and pollutant are positively charged.

In these conditions, the HO^{\cdot} radicals, which are highly useful in the oxidation of micropollutants, would be generated in a short time with the adsorption of O_3 on the catalyst surface. Adsorption of O_3 molecules by hydroxyl radical on the surface causes a

generation of intermediate species (OH_3^\bullet) and another radical on the catalyst surface. The produced intermediate (OH_3^\bullet) turns into reactive HO^\bullet radicals and O_2 in an in situ reaction. In parallel, the radical species on the catalyst surface would adsorb water molecules and produce reactive HO^\bullet radicals. Due to the non-selective behavior of HO^\bullet , it can oxidize almost all organic contaminants, which causes the high removal efficiency of micropollutants. Furthermore, based on the charge of micropollutants (pK_a), pulling of micropollutants or expelling of micropollutants on the catalyst surface might happen, and each of these conditions can affect removal efficiency. In this condition, the desorption of micropollutants from the catalyst would happen due to the repulsive electrostatic forces, which means the contaminants do not occupy the active surface sites, and pore blocking and associated fouling on the surface would be limited.

There are conditions that the catalyst is uncharged. Uncharged catalysts usually have hydroxyl radicals on the surface. Although these radicals are uncharged, they can be the starter part for O_3 decomposition. In the O_3 decomposition reaction chain, after the adsorption of O_3 on the surface, chemical bond stretching and breaking can happen in several ways. In one case, after bond breaking, HO^\bullet and O_2 would be generated directly. In another case, some intermediate species such as OH_3^\bullet and O_3^- would be produced. The produced intermediate (OH_3^\bullet) turns into reactive HO^\bullet radicals and O_2 in an in situ reaction. In parallel, O_3^- causes other chain reactions, which finally produce HO^\bullet . Figure 4 proposed influencing mechanisms when the catalyst is uncharged.

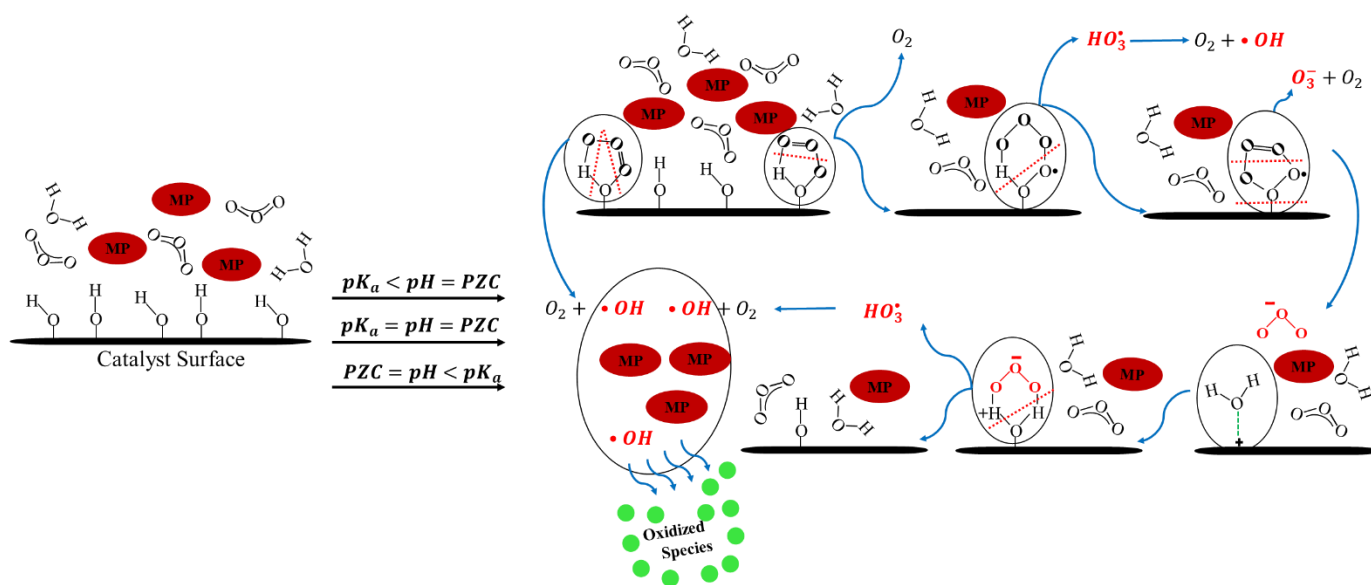


Figure 4. Proposed three influencing mechanisms using uncharged catalysts.

$\text{pK}_a < \text{pH}$, $\text{PZC} = \text{pH}$: Catalyst is uncharged, Pollutant is negatively charged.
 $\text{pH} < \text{pK}_a$, $\text{PZC} = \text{pH}$: Catalyst is uncharged, Pollutant is positively charged.
 $\text{PZC} = \text{pH} = \text{pK}_a$: Catalyst is uncharged, Pollutant is uncharged.

Due to the uncharged catalyst surface, there is no considerable difference between the three conditions in this subcategory.

Figure 5 summarizes three conditions related to the negatively charged surface of the catalyst. This situation seems to be the most favored for the adsorption and subsequent decomposition of O_3 .

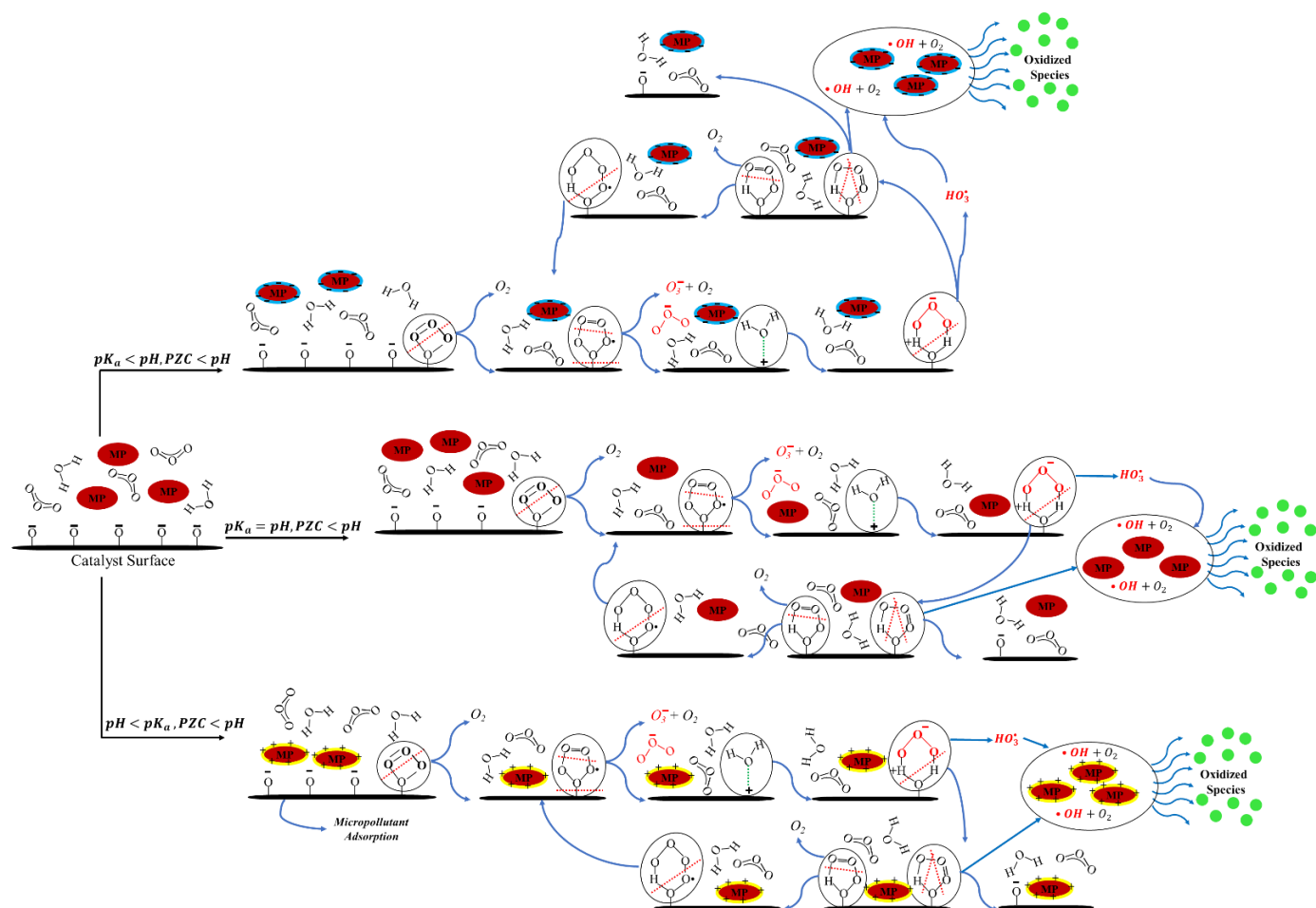


Figure 5. Proposed three influencing mechanisms using negatively charged catalysts.

In fact, the adsorption of O_3 on a surface would generate intermediate species such as O_3^- and OH_3^\bullet , considered as precursors of the high oxidant species HO^\bullet .

$PZC < pH < pK_a$: Catalyst is negatively charged, pollutant is positively charged.

Although in this condition, adsorption of O_3 is favored, adsorption of the pollutant on the catalyst surface can occur too. Thus, the pore blocking and associated fouling on the surface and reducing the active surface sites might have a negative effect on the HO^\bullet generation in the environment. On the other side, closing to the area of HO^\bullet radicals generation might cause quickly oxidize of micropollutants.

$PZC < pH, pH = pK_a$: Catalyst is negatively charged, pollutant is uncharged.

There is no effective interaction between the catalyst and micropollutants in this condition, so the generation of HO^\bullet by O_3 decomposition is the only effective parameter here.

$PZC < pH, pK_a < pH$: Catalyst and pollutant negatively charged.

In this condition, the negatively charged micropollutants would be repulsed from the negatively charged catalyst surface due to the electrostatic forces. Thus, the micropollutants do not occupy the active surface sites.

The values of pK_a for different pollutants reported in Table 3 have been examined in order to compare and better evaluate the fundamental mechanisms proposed in this section.

Table 3. Values of pKa for different pollutants.

Target Pollutants	pKa	Ref.	Target Pollutants	pKa	Ref.
Isoniazid	1.82	[49]	Ciprofloxacin (CPF)	6.38	[50]
Oxalic acid (OA)	pKa1 = 1.14; pKa2 = 3.64	[51]	4-nitrophenol	7.15	[52]
Phenacetin	2.2	[53]	Fluoxetine	8.7	[50]
Amoxicillin	2.4	[50]	Atenolol	9.16	[50]
Humic acids	2.5	[54]	Acetaminophen	9.38	[55]
Sulfamethazine	2.65	[50]	4-Chloro phenol	9.41	[52]
Salicylic acid	3.5	[50]	Paracetamol (PCT)	9.39–9.5	[50,56]
Methylene blue	3.8	[57]	4-Chloro-2-methyl	9.71	[52]
Reactive black-5	3.8	[58]	Phenol (PH)	9.98	[59]
Furosemide	3.9	[50]	m-cresol	10.1	[60]
Diclofenac	4.15	[50]	Bisphenol-A (BPA)	10.29	[61]
Naproxen	4.2	[50]	2,4-dimethylphenol	10.4	[52]
Ibuprofen	4.51	[50]	Orange (II)	11.4	[62]
Acetic acid	4.76	[63]	RR189	11.7	[64]
(SMX)	5.6–5.8	[65,66]	Carbamazepine	13.9	[50]
Naphthenic acid	5–6	[67]			

The PZC values for selected catalysts referring to the reviewed articles are shown in Table 4. Based on the type of catalysts, the pathway of the catalytic ozonation can also be varied. Although some catalysts exhibit PZC values in narrow ranges due to various impurity contents, synthesis routes, or thermal histories, this difference appears to be of little relevance to their catalytic properties.

Table 4. Range of PZC for selected catalysts.

Catalysts	PZC	Ref.	Catalysts	PZC	Ref.
SiO ₂	2.6	[68,69]	CoFe ₂ O ₄	7.31	[70]
MnO ₂	3–5	[1,71]	Fe ₃ O ₄ nanoparticles	7.4	[72]
MWCNTs	4.2	[68]	CeO ₂	8.1	[73]
α-Al ₂ O ₃	4.2	[74]	γ-Al ₂ O ₃	8.3–8.9	[75,76]
AC	4.9	[68]	NiO	8.45	[77]
NiCo ₂ O ₄	5	[78]	ZnO	9	[1]
FeOOH	5.9	[79]	α-Al ₂ O ₃	9.4	[75]
Ce ₃ O ₄	5–8	[69,80]	MgFe ₂ O ₄	9.8	[81]
CuFe ₂ O ₄	6–7	[53]	CuO	10	[82]
TiO ₂	6.2–6.6	[1]	MgO	12–13	[83]
Fe ₂ O ₃	6–9	[84]			

The main catalyst types applied in heterogeneous catalytic ozonation are metal/bimetal/polymetal oxides, metals or metal oxides on supports, and carbon-based materials. In each of these categories, the most popular catalysts and published works in recent years are summarized in this review.

4.1. Metal/Bimetal/Polymetal Oxides

Several metal oxides have been introduced to promote the heterogeneous catalytic ozonation processes. Some of these metal oxides are more popular than others in the catalytic ozonation process, such as Al₂O₃, MgO, CeO₂, MnO₂, NiO, ZnO, etc. Furthermore, some bimetal/polymetal oxides were widely applied due to their high stability as well as high catalytic activity, such as CuFe₂O₄, Mn-Ce-O, ZnAl₂O₄, etc. Table 5 compiles the literature results employing metal/bimetal/polymetal oxides for the degradation of pollutants in the catalytic ozonation process. As can be seen, operating conditions (pH, O₃ dosage, catalyst dose, etc.), the kind of used catalysts, target pollutants, and removal results are reported. The articles for summarizing in this part were chosen according to their high citations, and newness.

Table 5. Literature reports on different metal/bimetal/polymetal oxides as catalysts in the ozonation process (see Figures 3–5, respectively).

Catalysts	Target Pollutants	Operating Conditions		Removal Results	Year	Ref.
		pH < PZC	pH > pK _a , pH ≈ pK _a , pH < pK _a			
γ-Al ₂ O ₃ PZC = 8.9 +	Ibuprofen pK _a = 4.51 –	O ₃ dose: 0.5 mg/min; Catalyst dose: 5 g; pH: 7.2; T: 20 °C; t: 30 min		83% ibuprofen removal	2015	[76]
CoFe ₂ O ₄ PZC = 7.31 +	OA pK _{a1} = 1.14; pK _{a2} = 3.64	O ₃ dose: 14 ± 1 mg/L; Catalyst dose: 1 g/L; pH: 2.3; T: NR; t: 120 min		68.3% TOC removal	2017	[70]
γ-Al ₂ O ₃ PZC = 8.9 +	Cumene	O ₃ dose: 0.5 mg/min; Catalyst dose: 5 g; pH: 7.2; T: 20 °C; t: 30 min		58% cumene removal	2015	[76]
MgO PZC = 12–13 +	Methylene blue pK _a = 3.8 –	O ₃ dose 5 mg/L; Catalyst dose: NR; pH: 9; T: NR; t: 60 min		50% COD removal	2016	[85]
γ-Al ₂ O ₃ PZC = 8.9 +	1,2-dichlorobenzene	O ₃ dose: 0.5 mg/min; Catalyst dose: 5 g; pH: 7.2; T: 20 °C; t: 30 min		45% 1,2 dichlorobenzene removal	2015	[76]
γ-Al ₂ O ₃ PZC = 8.9 +	Acetic acid pK _a = 4.76 –	O ₃ dose: 0.5 mg/min; Catalyst dose: 5 g; pH: 7.2; T: 20 °C; t: 30 min		19% acetic acid removal	2015	[76]
Ce-O PZC = 8.5 +	CI Reactive Blue 5 (RB5)	O ₃ dose: 50 g/Nm ³ ; Catalyst dose: 350 mg; pH: 5.6; T: 25 °C; t: 3 h		85% TOC removal	2009	[86]
γ-Al ₂ O ₃ PZC = 8.3 +	Petroleum refinery wastewater	O ₃ dose: 5 mg/min; Catalyst dose: 0.5 g; pH: 8.15; T: 30 °C; t: 40 min		45.9% COD removal	2017	[87]
MgO PZC = 12–13 +	Acetaminophen pK _a = 9.38 +	O ₃ dose: 50 mg/L; Catalyst dose: 2 g/L; pH: 5.4; T: NR; t: 10 min		100% ACT degradation	2017	[16]
MgO PZC = 12–13 +	RR198 pK _a = 11.7 +	O ₃ dose: 0.2 g/h; Catalyst dose: 5 g/L; pH: 8; T: 23 °C; t: 9 min		100% RR198 removal	2009	[88]
MgO PZC = 12–13 +	4-Chloro phenol pK _a = 9.41 +	O ₃ dose: 2.5 mg/min; Catalyst dose: 1.0 g/L; pH: 6.2; T: NR; t: NR		99.5% removal efficiency	2015	[17]
β-FeOOH PZC = 5.9 +	4-Chloro phenol pK _a = 9.41 +	O ₃ dose: 28.24 mg/L; Catalyst dose: 1 g/L; pH: 3.5; T: NR; t: 40 min		99% removal efficiency	2015	[89]
γ-Al ₂ O ₃ PZC = 8.3–8.9 +	PCT pK _a = 9.39–9.5 +	O ₃ dose: 3 mg/min; Catalyst dose: 5 mg/L; pH: 7; T: NR; t: 9 min		98% PCT removal	2018	[90]
MgO PZC = 12–13 +	PH pK _a = 9.98 +	O ₃ dose: 0.25 g/h; Catalyst dose: 4 g/L; pH: 7; T: 25 °C; t: 80 min		96% PH removal, 70% COD removal	2010	[91]
γ-Al ₂ O ₃ PZC = 8.3–8.9 +	Fluoxetine pK _a = 8.7 +	O ₃ dose: 30 mg/L; Catalyst dose: 1 g/L; pH: 7; T: 25 °C; t: 17 min		86% Fluoxetine removal	2019	[92]
MgFe ₂ O ₄ PZC = 9.8 +	Acid Orange II pK _a = 11.4 +	O ₃ dose: 5 mg/L; Catalyst dose: 0.5 mmol/L; pH: 4.6–9.6; T: 25 °C; t: NR		90% degradation efficiency	2016	[81]
NiO PZC = 8.45 +	Carbamazepine pK _a = 13.9 +	O ₃ dose: 5.5 g/m ³ ; Catalyst dose: 500 mg/L; pH: 3,4; T: 25 °C; t: 5 min		79.2% TOC removal	2020	[93]
CeO ₂ PZC = 8.1 +	SMX pK _a = 5.6–5.8 +	O ₃ dose: 50 g/Nm ³ ; Catalyst dose: 100 mg; pH: 4.8; T: NR; t: 3 h		61% TOC removal	2013	[94]
γ-Al ₂ O ₃ PZC = 8.3 +	2,4 dimethylphenol pK _a = 10.4 +	O ₃ dose: 2 g/Nm ³ ; Catalyst dose: 5 g/L; pH: 4.5; T: 25 °C; t: 300 min		57% TOC removal	2015	[95]
γ-Al ₂ O ₃ PZC = 8.3–8.9 +	Landfill leachate	O ₃ dose: 22 mg/min; Catalyst dose: 50 g/L; pH: 7.3; T: NR; t: 30 min		70% COD removal	2018	[96]
Al ₂ O ₃ PZC = 7.2–9.2 +	Textile wastewater	O ₃ dose: 0.9 mmol/L; Catalyst dose: 300 g; pH: 4; T: NR; t: NR		25.83% COD removal	2015	[97]

Table 5. Cont.

Catalysts	Target Pollutants	Operating Conditions		Removal Results	Year	Ref.
		pH \approx PZC	pH > pK _a , pH \approx pK _a , pH < pK _a			
NiCo ₂ O ₄ PZC = 5 N	Sulfamethazine pK _a = 2.65 —	O ₃ dose: 4.5 mg/min; Catalyst dose: 0.05 g/L; pH: 5.2; T: NR; t: 60 min		34.1% TOC removal	2021	[78]
α -MnO ₂ PZC = 3–5 N	4-Nitrophenol pK _a = 7.15 +	O ₃ dose: 20 mg/L; Catalyst dose: 100 mg, pH 3.5–5.9; T: NR; t: NR		96.7% degradation 79.5% TOC removal	2015	[98]
		pH > PZC	pH > pK _a , pH \approx pK _a , pH < pK _a			
α -Al ₂ O ₃ PZC = 4.2 —	Humic acids pK _a = 2.5 —	O ₃ dose: 0.063 m ³ /h; Catalyst dose: 0.5 g/L; pH: 5.5; T: 25 °C; t: 1 h		100% Humic acid removal	2020	[74]
γ -Al ₂ O ₃ PZC = 8.3–8.9 —	CPF pK _a = 6.38 —	O ₃ dose: 1.4 mg/L.min; Catalyst dose: 0.55 g/L; pH: 9.5; t: 60 min		93% removal efficiency	2019	[99]
Ca ₂ Fe ₂ O ₅ PZC = 9.5 —	Quinoline	O ₃ dose: 17 mg/L; Catalyst dose: 1 g; pH: 10.5; T: 25 °C; t: 120 min		92% COD removal	2022	[100]
CeO ₂ -MnO ₂ PZC = 10.13 —	Ammonium pK _a = 9.25 —	O ₃ dose: 12 mg/min; Catalyst dose: 1 g/L; pH: 11; T: NR; t: 60 min		88.14% Ammonium removal	2022	[101]
γ -Al ₂ O ₃ PZC = 8.3–8.9 —	Naphthenic acid pK _a = 5–6 —	O ₃ dose: NR; Catalyst dose: 1 g/L; pH: 8.5; T: 25 °C; t: 50 min		88% Naphthenic acids removal	2019	[102]
CuFe ₂ O ₄ PZC = 6–7 —	Phenacetin pK _a = 2.2 —	O ₃ dose: 0.36 mg/L; Catalyst dose: 2.0 g/L; pH: 7.72; T: NR; t: 30 min		95% of degradation	2015	[53]
α -MnO ₂ PZC = 3–5 —	BPA pK _a = 10.29 +	O ₃ dose: 4.47 mmol/min; Catalyst 0.1 mg/L; pH: 6.25; T: 20 °C; t: NR		93.5% removal efficiency	2015	[103]

NR—value not reported, TOC—total organic carbon, COD—chemical oxygen demand.

In Table 5, the PZC values of the metal oxide catalysts with the pK_a of the pollutants in different operating conditions are correlated in order to identify the most favorable combinations for their removal.

From this comparison, it can be seen that the best removal efficiency trend is provided for experimental pH values in which the catalyst surface is charged. The electrostatic repulsion between pollutant and catalyst allows rapid O₃ decomposition, as well as the formation of radical species that occurs in the proximity of the pollutant adsorbed on the surface of the catalyst, seem to be the most effective mechanisms.

Al₂O₃ is one of the most popular materials in the catalytic ozonation process, among which several studies performed at pH close to neutral confirm it as a catalyst with excellent removal yields. The PZC value of Al₂O₃ can be different due to the catalyst's various impurities content, synthesis route, or thermal history, but the approximate range of PZC value is 7.2–9.4 [75,90,97]. Scrutinizing the study of Ziylan-Yavaş et al. [90] that had more than 95% removal of PCT (pK_a \approx 9.5 (Table 3)) by using γ -Al₂O₃ (PZC = 8.3–8.9 (Table 4)) as a catalyst verified that the optimal condition was when pH of the solution was lower than pK_a and PZC. In these conditions, both catalyst and pollutant are positively charged. So, the governing mechanism was the repulsive electrostatic forces resulting in the desorption of the micropollutant from the catalyst which does not occupy the active surface sites, favoring the O₃ adsorption and its decomposition. Nemati Sani et al. [99] studied the catalytic efficiency of Al₂O₃ for CPF degradation in the catalytic ozonation process. Based on their work, the highest removal efficiency was at pH = 9.5. In this condition PZC < pH, pK_a < pH, which means both catalyst and pollutant are negatively charged. So, as previously mentioned, in this condition there is not any effective adsorption of pollutants on the surface of the catalyst, and the primary mechanism is related to O₃ decomposition. In explaining their work, they clearly mentioned that ozonation is responsible for 88% of the CPF removal efficiency, which is another proof of the accurate understanding of govern mechanism categories in this review.

MgO is another efficient metal oxide that had excellent results in micropollutants degradation. The PZC value of MgO is in the range of 12–13 approximately [83]. With this PZC in a wide range of solution pH, MgO is positively charged. So oxidation of micropollutants due to the generation of HO• radicals in the solution is the governing mechanism for catalytic ozonation by using this metal oxide. Based on using MgO as a catalyst, several works with considerable target pollutants removal are reported. Mashayekh-Salehi et al. [16] achieved complete degradation of acetaminophen in only 10 min of reaction time in the catalytic ozonation process. Based on our categorization, this work is in $\text{pH} < \text{PZC}$, $\text{pH} < \text{pK}_a$ condition. So, as previously mentioned, there is no effective adsorption of pollutants on the catalyst's surface due to the similar charges (positive charges). The primary mechanism is related to the oxidation of micropollutants due to the generation of HO• radicals in the solution. It is worth mentioning, the authors confirmed that the reaction with HO• radical was the leading cause of ACT oxidation using the MgO/O₃ process. The same condition ($\text{pH} < \text{PZC}$, $\text{pH} < \text{pK}_a$) was applied by Moussavi et al. [88], Kong et al. [17], and Mousavi et al. [91]. The exciting results of comparing these works was that they all achieved more than 95% degradation of their target pollutant, which is almost the top result for the catalytic ozonation process. This observation may prove that MgO is one of the best catalysts for the ozonation process, and this condition ($\text{pH} < \text{PZC}$, $\text{pH} < \text{pK}_a$) may be one of the best catalytic ozonation conditions, especially for the removal of very weak acid pollutants.

Furthermore, some scientists indicated that the catalytic mechanism and removal efficiency highly depend on the catalyst's characteristics. In this regard, introducing bimetal/polymetal oxides and using different synthesis routes with better chemical and physical properties was another way of improving this field. The proposed catalytic ozonation mechanisms are also rationalized for these kinds of catalysts. Oputu et al. [89] studied catalytic ozonation activity using β -FeOOH as a catalyst and 4-chloro phenol as the target pollutant. The pH of the solution was 3.5, so based on reported PZC (Table 4) and pK_a (Table 3), both the pollutant and catalyst surface was a positive charge. According to the governing mechanism, the O₃ adsorption then its decomposition are favored, and there is no adsorption of pollutants on the surface due to the same positive charges. The interesting results based on this work were that in the presence of O₃ and catalyst, the removal efficiency was 99% (almost complete removal); however, in the absence of O₃, using only catalyst, the removal efficiency was 3%. This thought-provoking achievement shows that O₃ decomposition is the main effecting parameter in this condition; furthermore, the effect of pollutant adsorption on the catalyst surface is negligible.

Other metal oxide catalysts need to be mentioned, such as magnetic Fe₃O₄ nanoparticles [104] and δ -MnO₂ [105]. These metal oxides have shown good removal efficiencies but have not been reported in Table 5 as their pH values are not reported in the articles so their unclear process conditions do not allow to frame them in the proposed mechanism.

After perusing a lot of published articles from previous years, it is important to highlight that due to a large number of studies on these materials and the development of our understanding and knowledge about them, these materials can now be used for real wastewater plants. By scrutinizing the trend of published articles, changes in applications from laboratory scale to real wastewater plant can be observed.

4.2. Metal/Metal Oxides on Supports

This kind of catalyst was prepared by loading metal or metal oxides on supporters with unique surface properties due to increasing the catalytic activity of metal/metal oxides in the ozonation process. By applying this kind of material, both the surface area and the active sites of the materials would be increased. By the combination of metals/metal oxides and supporters, the PZC value of the prepared catalyst shifts to more acidic/basic, resulting in a new PZC value. This PZC change is attributed to the complexation of loaded metal/metal oxides onto the support surface. So, the kind of loading materials is important in this case. The following will clarify the governing mechanisms by scrutinizing several

related articles in this field. Table 6 systemizes the literature that employed metal/metal oxides as supports for the degradation of pollutants in the catalytic ozonation process. Operating conditions (pH, O₃ dosage, catalyst dose, etc.), the catalysts used, target pollutants, and removal results are reported.

Table 6. Literature reports on different metals/metal oxides on support as catalysts in the ozonation process (see Figures 3–5, respectively).

Catalysts	Target Pollutants	Operating Conditions		Removal Results	Year	Ref.
		pH < PZC	pH > pK _a , pH ≈ pK _a , pH < pK _a			
Ce _{1.0} Fe _{0.9} OOH PZC = 7.8 +	Sulphamethazine pK _a = 2.65 –	O ₃ dose: 15 mg/L; Catalyst dose: 0.2 g/L; pH: 7.3; T: NR; t: 15 min		41.2% mineralization efficiency	2016	[106]
LaTi _{0.15} Cu _{0.85} O ₃ PZC = 9.8 +	SMX pK _a = 5.6–5.8 –	O ₃ dose: 25 mg/L; Catalyst dose: NR; pH: 7; T: 20 °C; t: 2 h		85% TOC removal	2009	[107]
Ce deposited magnetic pyrite cinder PZC = 7.63 +	Reactive black-5 pK _a = 3.8 –	O ₃ dose 5.6 mg/min; Catalyst dose: 2.5 g/L; pH: 5.5; T: NR; t: 2 h		83.32% TOC removal efficiency	2016	[69]
Ca-C/Al ₂ O ₃ PZC = 9.53 +	High-salt organic wastewater	O ₃ dose: 12 mg/L; Catalyst dose: 20 g; pH: 8.36; T: NR; t: 40 min		64.4% COD removal efficiency	2022	[108]
Mn-CeOx@γ-Al ₂ O ₃ PZC = 9.37 +	CPF pK _a = 6.38 –	O ₃ dose: 13.969 ± 0.434 mg/L; Catalyst dose: 80 g/L; pH: 8.5; T: NR; t: 60 min		100% CPF removal	2022	[109]
Mg-doped ZnO PZC = 11–11.2 +	Isoniazid pK _a = 1.82 –	O ₃ dose: 10–25 mg/L; Catalyst dose: 0.1 g/L; pH: 7.2; T: NR; t: 9 min		76.3% removal efficiency	2020	[49]
MnOx/SBA-15 PZC = 4.27–6.35 +	Clofibric acid pK _a = 3.2 –	O ₃ dose: 1 mg/L; Catalyst dose: 0.2 g/L; pH: 3.85; T: 293 K; t: 15 min		43.8% TOC removal	2015	[20]
Fe-SBA-15 PZC = 4.0 +	OA pK _{a1} = 1.14; pK _{a2} = 3.64 N/–	O ₃ dose: 100 mg/h; Catalyst dose: 0.24 g; pH: 3; T: NR; t: 60 min		86.6% removal efficiency	2016	[21]
Fe-MCM-41 PZC = 4.95 +	OA pK _{a1} = 1.25; pK _{a2} = 3.81 N/–	O ₃ dose: 21.8 mg/L; Catalyst dose: 0.4 g; pH: 3.6; T: NR; t: 30 min		94% degradation 6% TOC/TOC ₀ reduction	2017	[110]
SnOx-MnOx@Al ₂ O ₃ PZC = 8.7 +	PH pK _a = 9.98 +	O ₃ dose: 6 mg/L.min; Catalyst dose: 40 g/L; pH: 7; T: 20 ± 5 °C; t: 240 min		93.8% COD removal efficiency	2022	[111]
		pH ≈ PZC	pH > pK _a , pH ≈ pK _a , pH < pK _a			
4%Mn/γ-Al ₂ O ₃ PZC = 6.75 N	PH pK _a = 9.98 +	O ₃ dose: 8 mg/min; Catalyst dose: 0.20 g; pH: 6.5; T: 15 °C; t: NR		82.67% degradation efficiency	2016	[18]
MnOx-0.013/KCC-1 PZC = 4.0 N	OA pK _{a1} = 1.14; pK _{a2} = 3.64 –	O ₃ dose: 20 mg/L; Catalyst dose: 0.25 g/L; pH: 3.8; T: 25 °C; t: NR		86% TOC removal	2016	[112]
γ-Ti-Al ₂ O ₃ PZC = 7.3 N	SMX pK _a = 5.6–5.8 –	O ₃ dose: 30 mg/Nm ³ ; Catalyst dose: 1.5 g; pH: 7; T: NR; t: 1 h		92% TOC removal	2017	[113]
		pH > PZC	pH > pK _a , pH ≈ pK _a , pH < pK _a			
Cu–O–Mn/γ-Al ₂ O ₃ (CMA) PZC = 7.9 –	Polyvinyl alcohol pK _a = 5–6.5 –	O ₃ dose: 5.52 mg/L.min; Catalyst dose: 150 mg/L; pH: 10; T: 25 °C; t: 10 min		99.3% PVA removal	2020	[19]
Fe-MCM-41 PZC = 4.85 –	Diclofenac pK _a = 4.15 –	O ₃ dose: 100 mg/h; Catalyst dose: 1 g/L; pH: 7; T: NR; t: 30 min		76.3% mineralization 70% TOC reduction	2016	[114]
Cu/Al ₂ O ₃	Herbicide Alachlor	O ₃ dose: 12.2 mg/L.min; Catalyst dose: 0.27 g/L; pH: 4.4; T: 20 °C; t: NR		75% TOC removal	2013	[115]
FeMn-MCM-41	methyl orange	O ₃ dose: 35 mg/L; Catalyst dose: 0.2 g; pH: 7; T: 25 °C; t: NR		78% TOC removal	2021	[116]
MnOx/SBA-15 PZC = 5.33–6.06	Norfloxacin	O ₃ dose: 100 mg/h; Catalyst dose: 0.1 g/L; Catalyst loading 2%; pH: 5; T: 298 K; t: 60 min		54% mineralization efficiency	2017	[117]

Table 6. Cont.

Catalysts	Target Pollutants	Operating Conditions	Removal Results	Year	Ref.
MnO ₂ /Al ₂ O ₃	Quinoline	O ₃ dose: 135 mg/L; Catalyst dose: 70 g/L, 8% MnO ₂ loading; pH: NR; T: NR; t: 90 min	95% quinoline removal 65% TOC removal	2021	[118]
Fe silicate-loaded pumice	Diclofenac pKa = 4.15	O ₃ dose: 5 g/L; Catalyst dose: 8 g/L; pH 5; t: 30 min	73.3% mineralization 21.17% TOC removal	2017	[119]
MOF-derived Co ₃ O ₄ -C composite	Norfloxacin	O ₃ dose: 15 mg/L; Catalyst dose: 0.05 g/L; pH: 6.7; T: NR; t: NR	48% TOC removal	2021	[25]
Fe silicate doped FeOOH	p-Chloronitro benzene	O ₃ dose: 0.6 mg/L; Catalyst dose: 500 g/L; pH: 7; T: NR; t: 15 min	61.3% TOC removal	2017	[120]
Ni/NHPC	linear alkylbenzene sulfonate	O ₃ dose: NR; Catalyst dose: 0.3 g; pH: 10; T: NR; t: 30 min	98.1% LAS removal	2021	[121]
CuO/SiO ₂	Oxalate	O ₃ dose: 4 mg/L; Catalyst dose: 0.5 g, 4.5% metal loading; pH: 7; T: NR; t: NR	95% oxalate removal	2019	[122]
Pt-Al ₂ O ₃	PCT pKa = 9.4–9.5	O ₃ dose: 6 mg/L; Catalyst dose: 5 mg/L; pH: 7; T: NR; t: 5 min	100% PCT removal	2018	[90]
MnO ₂ /CeO ₂	Sulfosalicylic acid	O ₃ dose: 4 mg/min; Catalyst dose: 0.1 g; pH: 6.5; T: NR; t: 30 min	97% TOC removal	2016	[123]
Fe ₃ O ₄ /Co ₃ O ₄	SMX pKa = 5.6–5.8	O ₃ dose: 6 mg/L; Catalyst dose: 0.1 g/L; pH: 5.1; T: 25 °C; t: NR	60% TOC	2019	[124]
Mn-Ce-O	SMX pKa = 5.6–5.8	O ₃ dose: 120 mg/h; Catalyst dose: 1 g/L; pH: 6.9; T: NR; t: 120 min	69% COD removal	2015	[125]
CuO/Al ₂ O ₃ -EPC	SMX pKa = 5.6–5.8	O ₃ dose: 4.75 μM; Catalyst dose: 0.5 g/L; pH: 6.2; T: 20 °C; t: 15 min	87% SMX removal 21.2% TOC removal	2019	[126]
Fe ²⁺ -Montmorillonite	SMX pKa = 5.6–5.8	O ₃ dose: 5 mg/min; Catalyst dose: 1 g/L; pH: 2.88; T: NR; t: 20 min	97% COD removal	2015	[127]

NR—value not reported, TOC—total organic carbon, COD—chemical oxygen demand.

Wang et al. [18] studied the enhancement of PH removal in the catalytic ozonation process by introducing an Mn-doped Al₂O₃ nanocatalyst. Based on the Mn weight ratios (2 wt.% Mn/γ-Al₂O₃, 4 wt.% Mn/γ-Al₂O₃, 8 wt.% Mn/γ-Al₂O₃), the PZC values were measured. The study showed that by increasing the amount of loaded Mn, the PZC values of the catalyst decreased from 7.31 to 6.75 to 5.54, respectively. Studying the effect of Mn loaded, they observed that at the natural pH (pH = 6.5), 4 wt.% Mn/γ-Al₂O₃ showed the best efficiency on PH (pKa ≈ 9.98 (Table 3)) removal. It means O₃ decomposition is happening in the environment according to our suggested mechanism. Yan et al. [19] used γ-Al₂O₃ support but with another modification of the surface. In this study, Cu–O–Mn/γ-Al₂O₃ was used as a catalyst in the ozonation system for the degradation of polyvinyl alcohol. Based on their investigation related to PZC measurement, the PZC of γ-Al₂O₃ decreased from 8.4 to 7.9 after loading Cu and Mn. They mentioned that the optimal condition is when the PZC of the catalyst and pH of the solution are the same or the pH is more than PZC. In these conditions, the governing mechanism is related to the existing hydroxyl groups on the surface of the catalyst, the decomposition of O₃, and the generation of reactive oxidation species. In another work, Bing et al. [113] studied the mineralization of pharmaceuticals over γ-Ti-Al₂O₃ catalyst. The exciting part related to this article was scanning the surface reaction mechanism. Using in situ Raman spectroscopy, they characterized intermediate species formed on the γ-Ti-Al₂O₃ surface with an aqueous O₃ solution. They observed the appearance of two new peaks at 880 and 930 cm⁻¹ in γ-Ti-Al₂O₃ suspension with O₃, which were related to surface peroxide (O₂[•]) and surface atomic oxygen species (O[•]), respectively. As mentioned before in the governing mechanism explanation, these species would generate when the PZC of the catalyst is the same as the pH of the solution. They reported that the PZC value for this synthesized catalyst was 7.3 and the pH of the solution was 7. This work is an excellent observation for reliability even the details on intermediate species of our proposed govern mechanism.

One of the prominent supporting materials for catalysts is silica-based materials (such as SiO₂, SBA-15, MCM-41, etc.) due to their large surface area, good flexibility, stability,

adjustable structure, and biocompatibility. The following examples comprehensively illustrate the diversity of using these materials in catalytic ozonation.

Jeirani et al. [110] worked on a modified mesoporous Fe-MCM-41 catalyst to remove OA as a target pollutant. Their evaluation of the adsorption and ozonation process and the determination of PZC and pKa was thought-provoking. They specifically describe the dissociation of OA in water. OA (target pollutant) was ionized to hydrogen-oxalate anion ($C_2O_4H^-$), having a negative charge on the surface. On the other hand, the PZC value for Fe-MCM-41 and Mn, Ce/Fe-MCM-41 were measured (4.95 and 6, respectively); accordingly, the catalyst's surface was positively charged ($pH < PZC$). Then by comparing the adsorption and ozonation efficiency of the catalyst, they observed that adsorption was the governing mechanism for this treatment system, which is in line with our previous explanation of the mechanism.

Yan et al. [21] applied another silica-based material for OA removal. They found Fe-doped SBA-15 ($PZC = 4$) as a potential catalyst for the catalytic ozonation process. They studied the influence of initial pH in the range of 1 to 9 on the removal process. Based on their results and the known information about the pKa value of OA and PZC value of Fe-SBA-15, the best pH was 3 with 97.4% OA removal efficiency. This achievement affirms that the negatively charged micropollutants adsorbed on the positively charged catalyst surface. Thus, the contaminants were near where the generation of $\bullet OH$ radicals happens, which means $\bullet OH$ can quickly oxidize them in the environment. This mechanism is similar to the previous example of OA removal from wastewater.

Shen et al. [49] studied a new Mg-doped ZnO catalyst. By modifying the catalyst surface, the value of PZC was changed from 8 for ZnO support to 11.2 for the Mg-ZnO catalyst. Furthermore, by increasing the doping amount of Mg, the PZC value was increased. Interestingly, by changing the pH value from 3 to 9, the efficiency of the catalyst did not noticeably change because all of those pH values were less than the PZC of the catalyst ($pH < PZC$), so the reaction mechanism for all of those conditions were the same. Furthermore, their explanations related to the catalytic mechanism, surface charge, and kind of active radicals were another validation of our suggested governing mechanism.

For many of these supported catalysts, the lack of studies on the new PZC values makes it difficult to predict their mechanism of action, although they show high removal efficiency as reported in Table 6.

4.3. Carbon-Based Materials

Applying carbon-based materials has received significant popularity in the catalytic ozonation process during past decades. The variety of these materials, their good catalytic performance, and their environmentally friendly properties make them very attractive for these studies. Bulky carbons (such as activated carbon (AC)), nano carbons (such as carbon nanotubes (CNTs) and graphene), and carbon-based nanocomposites are the three most popular materials in catalytic ozonation. Table 7 compiles the literature results employing carbon-based materials for the degradation of organics. As can be seen, the systems have been investigated over a wide range of operating conditions (pH, O_3 dosage, the mass ratio between solid and organic matter load, etc.), the kind of used catalysts, target pollutants, and removal results. The articles for summarizing this part were chosen according to their high citations.

Table 7. Literature reports on different carbon-based materials as catalysts in the ozonation process (see Figures 3–5, respectively).

Catalysts	Target Pollutants	Operating Conditions		Removal Results	Year	Ref.
		pH < PZC	pH > pK _a , pH ≈ pK _a , pH < pK _a			
Fe/AC PZC = 7.95 +	Crystal violet dye pKa1 = 1.15 pKa2 = 1.8 –	O ₃ dose: 4.44 mg/min; Catalyst dose: 2.5 g/L; pH: 7; T: NR; t: NR		>96% decolorization	2015	[128]
AC PZC = 8.5 +	SMX pKa = 5.6–5.8 +	O ₃ dose: 50 g/Nm ³ ; Catalyst dose: 100 mg; pH: 4.8; T: NR; t: 3 h		45% TOC removal	2011	[129]
AC PZC = 8.5 +	SMX pKa = 5.6–5.8 +	O ₃ dose: 48 mg/L; Catalyst dose: 2 g/L; pH: 5; T: 26 °C; t: 20 min		78% TOC removal	2011	[130]
Treated Commercial MWCNT-HNO ₃ -N ₂ -900 PZC = 7.3 +	SMX pKa = 5.6–5.8 +	O ₃ dose: 50 g/Nm ³ ; Catalyst dose: 100 mg; pH: 4.8; T: NR; t: 3 h		45% TOC removal	2013	[131]
Treated Commercial MWCNT-O ₂ PZC = 5.2 +	SMX pKa = 5.6–5.8 +	O ₃ dose: 50 g/Nm ³ ; Catalyst dose: 100 mg; pH: 4.8; T: NR; t: 3 h		41% TOC removal	2013	[131]
MWCNT PZC = 7 +	SMX pKa = 5.6–5.8 +	O ₃ dose: 50 g/Nm ³ ; Catalyst dose: 100 mg; pH: 4.8; T: NR; t: 3 h		35% TOC removal	2011	[130]
AC ₀ PZC = 8.5 +	RB5	O ₃ dose: 50 g/Nm ³ ; Catalyst dose: 350 mg; pH: 5.6; T: 25 °C; t: 2 h		70% TOC removal	2009	[86]
AC ₀ -Ce-O composite PZC = 8.5 +	RB5	O ₃ dose: 50 g/Nm ³ ; Catalyst dose: 350 mg; pH: 5.6; T: 25 °C; t: 2 h		100% TOC removal	2009	[86]
		pH ≈ PZC	pH > pK _a , pH ≈ pK _a , pH < pK _a			
MnOx/sewage sludge-derived AC PZC = 3.5 N	OA pKa1 = 1.14; pKa2 = 3.64 N/–	O ₃ dose: 5 mg/L; Catalyst dose: 100 mg/L, Catalyst loading 30%; pH: 3.5; T: NR; t: 60 min		92.2% removal efficiency	2017	[132]
Fe-MnOx/AC PZC = 6.1 N	PH pKa = 9.9 +	O ₃ dose: 60 mg/L; Catalyst dose: 1 g/L; pH: 6; T: NR; t: 20 min		90.75% TOC removal	2022	[133]
		pH > PZC	pH > pK _a , pH ≈ pK _a , pH < pK _a			
AC Darco 12–20 PZC = 6.4 –	SMX pKa = 5.6–5.8 –	O ₃ dose: 25 mg/L; Catalyst dose: NR; pH: 7; T: 20 °C; t: 2 h		92% TOC removal	2012	[107]
AC/nano-Fe ₃ O ₄ PZC = 6.08–7.7 –	PH pKa = 9.9 +	O ₃ dose: 33 mg/L.min; Catalyst dose: 2 g/L; pH: 8; T: NR; t: 60 min		98.5% PH removal 69.8% COD removal	2014	[134]
CeO ₂ /MWCNT	SMX	O ₃ dose: 50 g/Nm ³ ; Catalyst dose: 100 mg; pH: 4.8; T: NR; t: 3 h		56% TOC removal	2013	[94]
Fe ₂ O ₃ /CeO ₂ loaded AC (MOPAC)	SMX	O ₃ dose: 48 mg/L; Catalyst dose: 2 g/L; pH: 5; T: 26 °C; t: 20 min		86% TOC removal	2011	[130]
rGO	p-Hydroxybenzoic Acid (PHBA)	O ₃ dose: 20 mg/L; Catalyst dose: 0.1 g/L mg; pH: 3.5; T: 25 °C; t: 30 min		100% PHBA removal	2016	[135]
α-MnO ₂ /RGO	BPA	O ₃ dose: 4.47 mmol/min; Catalyst dose: 0.1 mg/L; pH: 6.25; T: 20 °C; t: 60 min		90.5% BPA removal	2015	[103]
GO/Fe ₃ O ₄	ρ-chlorobenzoic acid (pCBA)	O ₃ dose: 4 mg/L; Catalyst dose: 20 mg/L; pH: 7; T: NR; t: 5 min		51% TOC removal	2018	[136]
Heteroatom doped graphene oxide PGO	SMX	O ₃ dose: 2 g/h; Catalyst dose: 1 g/L; pH: 9; T: 25 °C; t: 5 min		99% SMX removal	2017	[137]

NR—value not reported, TOC—total organic carbon, COD—chemical oxygen demand.

As it is apparent in Table 7, AC or carbon black is one of the most used catalysts for the ozonation process. High porosity, surface functionalities, its low cost are the reasons for its extensive utilization. The PZC value of AC can be different due to the catalyst's various impurities content, synthesis route, or thermal history, and the method for investigation of PZC, while the reported range of PZC value for AC is between 4.9–11.9 [68,138]. On the other hand, commercially available AC can be modified by minerals such as alkali metals

(Ca, Na, K, Li, Mg) or multivalent metals (Al, Fe, Ti, Si) and metal oxides. The presence of impurities on the surface of AC would significantly affect the PZC values. In most articles, the authors reported this value for the AC used in their work.

Shahamat et al. [134] studied a new carbon-based catalyst called AC/nano-Fe₃O₄ to remove PH. During this study, they calculated the PZC of the catalyst and illustrated that when the pH of the solution is between PZC and pK_a, the negative catalytic charge and positive charge of the pollutant can attract each other on the surface of the catalyst. O₃ decomposition is the primary reaction mechanism when the catalyst has a negative charge. These conditions were responsible for achieving the optimal efficiency for PH removal. In another work, Huang et al. [132] synthesized MnOx/sewage sludge-derived AC (MnOx/SAC) to improve the catalytic efficiency of OA degradation in ozonation. Based on the report, the best organic contaminant removal was at the pH equal to the PZC of the catalyst (PZC = 3.5), and the governing mechanism was related to existing hydroxyl radicals on the catalyst's surface which is the starter part for O₃ decomposition. Synthesized Fe-loaded AC for dibutyl phthalate removal was another work by Huang et al. [139], which had the same result that an uncharged surface with hydroxyl radicals on the surface was more active than the charged surface.

CNTs and MWCNTs are used frequently in the catalytic ozonation process as the mixed mesoporous structured nanocarbons. Acceleration of reaction kinetics, rapid mass diffusion, large surface area, and facile modification of surface are the main advantages of this kind of catalyst. Several techniques were used to promote the catalytic activity of this material, such as substituting carbon atoms with metal-free heteroatoms (e.g., N, S, and F).

Gonçalves et al. [131] studied the effect of MWCNTs on the catalytic ozonation of SMX (pK_a ≈ 5.6–5.8 (Table 3)). A set of modified MWCNTs with different levels of acidity/basicity was prepared and tested. The PZC value of the original MWCNT was 7; however, by modification of the original catalyst, the amount of PZC was changed to more acidic and basic. Based on the results, all those catalysts illustrated excellent efficiency for SMX removal, but one of the modified MWCNTs, called MWCNT-HNO₃_N₂_900 with PZC 7.3, illustrated better catalytic efficiency than the others. Based on our categorization and the observation in this work, at pH < PZC, pH < pK_a condition, there is no effective adsorption of pollutants on the catalyst's surface due to the similar charges (positive charges). So the primary mechanism is related to the oxidation of micropollutants due to the generation of HO• radicals in the solution.

Graphene oxide (GO) and reduced graphene oxide (rGO) are other prominent catalysts that have been extensively employed to accelerate the degradation of various contaminants by O₃. Scrutinizing the study of Wang et al. [135] that had complete PHBA removal (pK_a ≈ 4.85) by using rGO (PZC = 4.7) as a catalyst verified that the optimal condition was at the pH of 3.5. As mentioned before, in the condition that pH < PZC, pH < pK_a, both catalyst and pollutant are positively charged, which leads to no adsorption on the system so that the primary mechanism would be related to the generation of HO• by O₃ decomposition.

4.4. Metal–Organic Frameworks (MOFs)

As a rapidly emerging category of porous materials, metal–organic frameworks (MOFs) are widely used in different research fields due to their unique topology, adjustable features, large surface area, ultrahigh porosity, and ease of access to numerous functional groups [27,140–143]. The presence of hydroxyl groups on the surface of MOFs and the open metal sites of MOFs are two powerful catalytic active sites for the ozonation process. Their presence plays an important role in the adsorption and decomposition of O₃. The catalytic efficiency of MOF highly depends on the type of metal incorporated in the MOF. Therefore, there are several studies on designing and synthesizing MOFs to produce an appropriate catalyst to be used in the catalytic ozonation process [26,121,143–149]. In recent years, several studies have been reported on the applicability of MOFs in the catalytic ozonation process, including Co/Ni-MOF [150], Ce-doped MIL-88A(Fe) [26], and Fe-based

MOFs [151], and this emerging category of materials could be one of high-potential materials by considering some improvements in the future.

5. Conclusions

This review focused on a bibliometric study of catalytic ozonation as one of the popular AOPs methods, conducted from 2000–2021. Nearly 600 articles published during this period, identified by the Web of Science (WOS) database and a bibliometric analysis using VOS viewer software, have been carefully examined and evaluated in terms of future development and practicability. The most impacting articles have been scrutinized and discussed in terms of the interpretation of mechanism and a new vision outlined on the evaluation of both heterogeneously and homogeneously catalyzed ozonation processes for the degradation and mineralization of various toxic organic pollutants in water.

Particular attention has been devoted to describing the activities and efficiency of heterogeneous catalysts in the ozonation process related to the chemical properties of catalysts such as crystallographic and morphological, chemical stability as well as the opportune combination of their PZC values with pKa of the target pollutant and pH of the solution.

Examining the results related to the catalytic activity of the metal oxide catalysts, it can be emphasized that the best performance can be obtained when the PZC and pKa values produce positively charged catalyst surfaces and target pollutants, respectively. Despite the small number of citing works, the negatively charged pollutant and the catalyst surface seem a favorable combination for obtaining a good removal efficiency. At least for this type of heterogeneous catalyst, it can be assumed that the repulsion between the pollutants and catalysts promotes the formation of HO• as the species responsible for the enhancement of the removal processes of the target pollutant. Carbon-based catalysts do not seem to follow this trend; for this reason, deeper investigations could be expected for this class of materials in the future.

Finally, we believe that this study may be of help to authors aiming to improve knowledge in this field.

Author Contributions: Conceptualization, N.F. and E.B.; methodology, N.F.; software, N.F.; validation, N.F., E.B., D.S. and G.M.; formal analysis, N.F. and E.B.; investigation, N.F. and E.B.; resources, N.F. and E.B.; data curation, N.F. and E.B.; writing—original draft preparation, N.F.; writing—review and editing, N.F., E.B. and G.M.; visualization, D.S.; supervision, D.S. and G.M.; project administration, G.M.; funding acquisition, G.M. All authors have read and agreed to the published version of the manuscript.

Funding: PANIWATER project funded jointly by the European Union's Horizon 2020 research and innovation programme: 820718; Programma Operativo Nazionale Ricerca e Innovazione 2014–2020: F85F20000290007.

Data Availability Statement: Not applicable.

Acknowledgments: All individuals included in this section have consented to the acknowledgment.

Conflicts of Interest: The authors declare no conflict of interest.

References

1. Boczkaj, G.; Fernandes, A. Wastewater treatment by means of advanced oxidation processes at basic pH conditions: A review. *Chem. Eng. J.* **2017**, *320*, 608–633. [[CrossRef](#)]
2. Méndez-Arriaga, F.; Otsu, T.; Oyama, T.; Gimenez, J.; Esplugas, S.; Hidaka, H.; Serpone, N. Photooxidation of the antidepressant drug Fluoxetine (Prozac®) in aqueous media by hybrid catalytic/ozonation processes. *Water Res.* **2011**, *45*, 2782–2794. [[CrossRef](#)] [[PubMed](#)]
3. Kusic, H.; Koprivanac, N.; Bozic, A.L. Minimization of organic pollutant content in aqueous solution by means of AOPs: UV- and ozone-based technologies. *Chem. Eng. J.* **2006**, *123*, 127–137. [[CrossRef](#)]
4. Zangeneh, H.; Zinatizadeh, A.A.L.; Feizy, M. A comparative study on the performance of different advanced oxidation processes (UV/O₃/H₂O₂) treating linear alkyl benzene (LAB) production plant's wastewater. *J. Ind. Eng. Chem.* **2014**, *20*, 1453–1461. [[CrossRef](#)]

5. Lucas, M.; Peres, J.; Puma, G.L. Treatment of winery wastewater by ozone-based advanced oxidation processes (O_3 , O_3/UV and $O_3/UV/H_2O_2$) in a pilot-scale bubble column reactor and process economics. *Sep. Purify. Technol.* **2010**, *72*, 235–241. [[CrossRef](#)]
6. Gimeno, O.; Rivas, F.J.; Beltrán, F.J.; Carbajo, M. Photocatalytic Ozonation of Winery Wastewaters. *J. Agric. Food Chem.* **2007**, *55*, 9944–9950. [[CrossRef](#)] [[PubMed](#)]
7. Adil, S.; Maryam, B.; Kim, E.-J.; Dulova, N. Individual and simultaneous degradation of sulfamethoxazole and trimethoprim by ozone, ozone/hydrogen peroxide and ozone/persulfate processes: A comparative study. *Environ. Res.* **2020**, *189*, 109889. [[CrossRef](#)]
8. Urbina-Suarez, N.A.; Machuca-Martínez, F.; Barajas-Solano, A.F. Advanced Oxidation Processes and Biotechnological Alternatives for the Treatment of Tannery Wastewater. *Molecules* **2021**, *26*, 3222. [[CrossRef](#)]
9. Jiménez, S.; Andreozzi, M.; Micó, M.M.; Álvarez, M.G.; Contreras, S. Produced water treatment by advanced oxidation processes. *Sci. Total Environ.* **2019**, *666*, 12–21. [[CrossRef](#)]
10. Yang, Y.; Guo, H.; Zhang, Y.; Deng, Q.; Zhang, J. Degradation of Bisphenol A Using Ozone/Persulfate Process: Kinetics and Mechanism. *Water Air Soil Pollut.* **2016**, *227*, 53. [[CrossRef](#)]
11. Ding, P.; Chu, L.; Wang, J. Advanced treatment of petrochemical wastewater by combined ozonation and biological aerated filter. *Environ. Sci. Pollut. Res.* **2018**, *25*, 9673–9682. [[CrossRef](#)] [[PubMed](#)]
12. Wang, J.; Chen, H. Catalytic ozonation for water and wastewater treatment: Recent advances and perspective. *Sci. Total Environ.* **2020**, *704*, 135249. [[CrossRef](#)] [[PubMed](#)]
13. Azzouz, A.; Kotbi, A.; Niquette, P.; Sajin, T.; Ursu, A.V.; Rami, A.; Monette, F.; Hausler, R. Ozonation of oxalic acid catalyzed by ion-exchanged montmorillonite in moderately acidic media. *React. Kinet. Mech. Catal.* **2010**, *99*, 289–302. [[CrossRef](#)]
14. Afzal, S.; Quan, X.; Lu, S. Catalytic performance and an insight into the mechanism of CeO_2 nanocrystals with different exposed facets in catalytic ozonation of p-nitrophenol. *Appl. Catal. B Environ.* **2019**, *248*, 526–537. [[CrossRef](#)]
15. Nawrocki, J.; Kasprzyk-Hordern, B. The efficiency and mechanisms of catalytic ozonation. *Appl. Catal. B Environ.* **2010**, *99*, 27–42. [[CrossRef](#)]
16. Mashayekh-Salehi, A.; Moussavi, G.; Yaghmaeian, K. Preparation, characterization and catalytic activity of a novel mesoporous nanocrystalline MgO nanoparticle for ozonation of acetaminophen as an emerging water contaminant. *Chem. Eng. J.* **2017**, *310*, 157–169. [[CrossRef](#)]
17. Chen, J.; Tian, S.; Lu, J.; Xiong, Y. Catalytic performance of MgO with different exposed crystal facets towards the ozonation of 4-chlorophenol. *Appl. Catal. A Gen.* **2015**, *506*, 118–125. [[CrossRef](#)]
18. Wang, Y.; Yang, W.; Yin, X.; Liu, Y. The role of Mn-doping for catalytic ozonation of phenol using $Mn/\gamma-Al_2O_3$ nanocatalyst: Performance and mechanism. *J. Environ. Chem. Eng.* **2016**, *4*, 3415–3425. [[CrossRef](#)]
19. Yan, Z.; Zhu, J.; Hua, X.; Liang, D.; Dong, D.; Guo, Z.; Zheng, N.; Zhang, L. Catalytic ozonation for the degradation of polyvinyl alcohol in aqueous solution using catalyst based on copper and manganese. *J. Clean. Prod.* **2020**, *272*, 122856. [[CrossRef](#)]
20. Sun, Q.; Wang, Y.; Li, L.; Bing, J.; Wang, Y.; Yan, H. Mechanism for enhanced degradation of clofibric acid in aqueous by catalytic ozonation over $MnO_x/SBA-15$. *J. Hazard. Mater.* **2015**, *286*, 276–284. [[CrossRef](#)]
21. Yan, H.; Chen, W.; Liao, G.; Li, X.; Ma, S.; Li, L. Activity assessment of direct synthesized $Fe-SBA-15$ for catalytic ozonation of oxalic acid. *Sep. Purify. Technol.* **2016**, *159*, 1–6. [[CrossRef](#)]
22. Hong, W.; Zhu, T.; Sun, Y.; Wang, H.; Li, X.; Shen, F. Enhancing Oxygen Vacancies by Introducing Na^+ into OMS-2 Tunnels To Promote Catalytic Ozone Decomposition. *Environ. Sci. Technol.* **2019**, *53*, 13332–13343. [[CrossRef](#)] [[PubMed](#)]
23. Yang, L.; Hu, C.; Nie, Y. Surface acidity and reactivity of $\beta-FeOOH/Al_2O_3$ for pharmaceuticals degradation with ozone: In situ ATR-FTIR studies. *Appl. Catal. B Environ.* **2010**, *97*, 340–346. [[CrossRef](#)]
24. Wei, K.; Cao, X.; Gu, W.; Liang, P.; Huang, X.; Zhang, X. Ni-Induced $C-Al_2O_3$ -Framework ($NiCAF$) Supported Core–Multishell Catalysts for Efficient Catalytic Ozonation: A Structure-to-Performance Study. *Environ. Sci. Technol.* **2019**, *53*, 6917–6926. [[CrossRef](#)]
25. Chen, H.; Zhang, Z.; Hu, D.; Chen, C.; Zhang, Y.; He, S.; Wang, J. Catalytic ozonation of norfloxacin using Co_3O_4/C composite derived from ZIF-67 as catalyst. *Chemosphere* **2021**, *265*, 129047. [[CrossRef](#)]
26. Yu, D.; Wang, L.; Yang, T.; Yang, G.; Wang, D.; Ni, H.; Wu, M. Tuning Lewis acidity of iron-based metal-organic frameworks for enhanced catalytic ozonation. *Chem. Eng. J.* **2021**, *404*, 127075. [[CrossRef](#)]
27. Yu, D.; Li, L.; Wu, M.; Crittenden, J.C. Enhanced photocatalytic ozonation of organic pollutants using an iron-based metal-organic framework. *Appl. Catal. B Environ.* **2019**, *251*, 66–75. [[CrossRef](#)]
28. Sauleda, R.; Brillas, E. Mineralization of aniline and 4-chlorophenol in acidic solution by ozonation catalyzed with Fe^{2+} and UVA light. *Appl. Catal. B Environ.* **2001**, *29*, 135–145. [[CrossRef](#)]
29. Beltrán, F.J.; Rivas, F.J.; Montero-de-Espinosa, R. Iron type catalysts for the ozonation of oxalic acid in water. *Water Res.* **2005**, *39*, 3553–3564. [[CrossRef](#)]
30. Sánchez-Polo, M.; Rivera-Utrilla, J. Ozonation of 1,3,6-naphthalenetrisulfonic acid in presence of heavy metals. *J. Chem. Technol. Biotechnol.* **2004**, *79*, 902–909. [[CrossRef](#)]
31. Ramos, R.M.B.; Biz, A.P.; Tavares, D.A.; Kolichieski, M.B.; Dantas, T.L.P. Homogeneous Catalytic Ozonation of Lipids Involving Fe^{2+} and Mn^{2+} : An Experimental and Modeling Study. *CLEAN—Soil Air Water* **2020**, *48*, 1900430. [[CrossRef](#)]
32. Cortés, S.; Sarasa, J.; Ormad, P.; Gracia, R.; Ovelleiro, J.L. Comparative Efficiency of the Systems $O_3/High\ pH$ And $O_3/catalyst$ for the Oxidation of Chlorobenzenes in Water. *Ozone Sci. Eng.* **2000**, *22*, 415–426. [[CrossRef](#)]

33. Fu, P.; Wang, L.; Li, G.; Hou, Z.; Ma, Y. Homogenous catalytic ozonation of aniline aerofloat collector by coexisted transition metallic ions in flotation wastewaters. *J. Environ. Chem. Eng.* **2020**, *8*, 103714. [[CrossRef](#)]
34. Wu, C.-H.; Kuo, C.-Y.; Chang, C.-L. Homogeneous catalytic ozonation of C.I. Reactive Red 2 by metallic ions in a bubble column reactor. *J. Hazard. Mater.* **2008**, *154*, 748–755. [[CrossRef](#)]
35. Psaltou, S.; Karapatis, A.; Mitrakas, M.; Zouboulis, A. The role of metal ions on p-CBA degradation by catalytic ozonation. *J. Environ. Chem. Eng.* **2019**, *7*, 103324. [[CrossRef](#)]
36. Beltrán, F.J.; Rivas, F.J.; Montero-de-Espinosa, R. Ozone-Enhanced Oxidation of Oxalic Acid in Water with Cobalt Catalysts. 1. Homogeneous Catalytic Ozonation. *Ind. Eng. Chem. Res.* **2003**, *42*, 3210–3217. [[CrossRef](#)]
37. El-Raady, A.A.A.; Nakajima, T. Decomposition of Carboxylic Acids in Water by O₃, O₃/H₂O₂, and O₃/Catalyst. *Ozone Sci. Eng.* **2005**, *27*, 11–18. [[CrossRef](#)]
38. Petre, A.L.; Carbajo, J.B.; Rosal, R.; García-Calvo, E.; Letón, P.; Perdigón-Melón, J.A. Influence of water matrix on copper-catalysed continuous ozonation and related ecotoxicity. *Appl. Catal. B Environ.* **2015**, *163*, 233–240. [[CrossRef](#)]
39. Tachibana, Y.; Nogami, M.; Sugiyama, Y.; Ikeda, Y. Effect of Pd(II) Species on Decomposition Reactions of Pyrrolidone Derivatives by Ozone. *Ozone Sci. Eng.* **2012**, *34*, 359–369. [[CrossRef](#)]
40. Andreozzi, R.; Caprio, V.; Insola, A.; Marotta, R.; Tufano, V. The ozonation of pyruvic acid in aqueous solutions catalyzed by suspended and dissolved manganese. *Water Res.* **1998**, *32*, 1492–1496. [[CrossRef](#)]
41. Ma, J.; Graham, N.J.D. Degradation of atrazine by manganese-catalysed ozonation influence of radical scavengers. *Water Res.* **2000**, *34*, 3822–3828. [[CrossRef](#)]
42. Ma, J.; Graham, N.J.D. Preliminary Investigation of Manganese-Catalyzed Ozonation for the Destruction of Atrazine. *Ozone Sci. Eng.* **1997**, *19*, 227–240. [[CrossRef](#)]
43. Xiao, H.; Liu, R.; Zhao, X.; Qu, J. Enhanced degradation of 2,4-dinitrotoluene by ozonation in the presence of manganese(II) and oxalic acid. *J. Mol. Catal. A Chem.* **2008**, *286*, 149–155. [[CrossRef](#)]
44. Xiao, H.; Liu, R.; Zhao, X.; Qu, J. Effect of manganese ion on the mineralization of 2,4-dichlorophenol by ozone. *Chemosphere* **2008**, *72*, 1006–1012. [[CrossRef](#)] [[PubMed](#)]
45. Rivas, J.; Rodríguez, E.; Beltrán, F.J.; García-Araya, J.F.; Alvarez, P. Homogeneous Catalyzed Ozonation of Simazine. Effect of Mn(II) and Fe(II). *J. Environ. Sci. Health B* **2001**, *36*, 317–330. [[CrossRef](#)] [[PubMed](#)]
46. Xian, Y.; Wen, S.; Liu, J.; Deng, J.; Bai, S. Discovery of a new source of unavoidable ions in pyrite aqueous solutions. *Min. Metall. Explor.* **2013**, *30*, 117–121. [[CrossRef](#)]
47. Cao, S.; Cao, Y.; Ma, Z.; Liao, Y. Metal Ion Release in Bastnaesite Flotation System and Implications for Flotation. *Minerals* **2018**, *8*, 203. [[CrossRef](#)]
48. Kasprzyk-Hordern, B.M.; Ziólek; Nawrocki, J. Catalytic ozonation and methods of enhancing molecular ozone reactions in water treatment. *Appl. Catal. B Environ.* **2003**, *46*, 639–669. [[CrossRef](#)]
49. Shen, T.; Zhang, X.; Lin, K.-Y.A.; Tong, S. Solid base Mg-doped ZnO for heterogeneous catalytic ozonation of isoniazid: Performance and mechanism. *Sci. Total Environ.* **2020**, *703*, 134983. [[CrossRef](#)]
50. Bones, J.; Thomas, K.; Nesterenko, N.; Paull, B. On-line preconcentration of pharmaceutical residues from large volume water samples using short reversed-phase monolithic cartridges coupled to LC-UV-ESI-MS. *Talanta* **2006**, *70*, 1117–1128. [[CrossRef](#)]
51. Vasca, E.; Ferri, D.; Manfredi, C.; Torello, L.; Fontanella, C.; Caruso, T.; Orrù, S. Complex formation equilibria in the binary Zn²⁺-oxalate and In³⁺-oxalate systems. *Dalton Trans.* **2003**, *13*, 2698–2703. [[CrossRef](#)]
52. Svobodová Vařeková, R.; Geidl, S.; Ionescu, C.-M.; Skřehota, O.; Kudera, M.; Sehnal, D.; Bouchal, T.; Abagyan, R.; Huber, H.J.; Koča, J. Predicting pKa Values of Substituted Phenols from Atomic Charges: Comparison of Different Quantum Mechanical Methods and Charge Distribution Schemes. *J. Chem. Inf. Model.* **2011**, *51*, 1795–1806. [[CrossRef](#)] [[PubMed](#)]
53. Qi, F.; Chu, W.; Xu, B. Ozonation of phenacetin in associated with a magnetic catalyst CuFe₂O₄, The reaction and transformation. *Chem. Eng. J.* **2015**, *262*, 552–562. [[CrossRef](#)]
54. Paul, S.; Sharma, T.R.; Saikia, D.; Saikia, P.; Borah, D.; Baruah, M.K. Evaluation of pKa Values of Soil Humic Acids and their Complexation Properties. *Int. J. Plant Soil Sci.* **2015**, *6*, 218–228. [[CrossRef](#)] [[PubMed](#)]
55. Lim, E.-B.; Vy, T.A.; Lee, S.-W. Comparative release kinetics of small drugs (ibuprofen and acetaminophen) from multifunctional mesoporous silica nanoparticles. *J. Mater. Chem. B* **2020**, *8*, 2096–2106. [[CrossRef](#)] [[PubMed](#)]
56. Bernal, V.; Erto, A.; Giraldo, L.; Moreno-Piraján, J.C. Effect of Solution pH on the Adsorption of Paracetamol on Chemically Modified Activated Carbons. *Molecules* **2017**, *22*, 1032. [[CrossRef](#)]
57. Sousa, H.R.; Silva, L.S.; Sousa, A.A.; Sousa, R.R.M.; Fonseca, M.G.; Osajima, J.A.; Silva-Filho, E.C. Evaluation of methylene blue removal by plasma activated palygorskites. *J. Mater. Res. Technol.* **2019**, *8*, 5432–5442. [[CrossRef](#)]
58. Karatay, S.E.; Aksu, Z.; Özeren, İ.; Dönmez, G. Potentiality of newly isolated *Aspergillus tubingensis* in biosorption of textile dyes: Equilibrium and kinetic modeling. *Biomass Convers. Biorefinery* **2021**, *155*, 1–8. [[CrossRef](#)]
59. Liptak, M.D.; Gross, K.C.; Seybold, G.; Feldgus, S.; Shields, G.C. Absolute pKa Determinations for Substituted Phenols. *J. Am. Chem. Soc.* **2002**, *124*, 6421–6427. [[CrossRef](#)]
60. Shiu, W.-Y.; Ma, K.-C.; Varhaníčková, D.; Mackay, D. Chlorophenols and alkylphenols: A review and correlation of environmentally relevant properties and fate in an evaluative environment. *Chemosphere* **1994**, *29*, 1155–1224. [[CrossRef](#)]

61. Corrales, J.; Kristofco, L.A.; Steele, W.B.; Yates, B.S.; Breed, C.S.; Williams, E.S.; Brooks, B.W. Global Assessment of Bisphenol A in the Environment: Review and Analysis of Its Occurrence and Bioaccumulation. *Dose-Response* **2015**, *13*, 1559325815598308. [[CrossRef](#)] [[PubMed](#)]
62. Dükkancı, M.; Vinatoru, M.; Mason, T.J. The sonochemical decolourisation of textile azo dye Orange II: Effects of Fenton type reagents and UV light. *Ultrason. Sonochem.* **2014**, *21*, 846–853. [[CrossRef](#)] [[PubMed](#)]
63. Goldberg, R.N.; Kishore, N.; Lennen, R.M. Thermodynamic Quantities for the Ionization Reactions of Buffers. *J. Phys. Chem. Ref. Data* **2002**, *31*, 231–370. [[CrossRef](#)]
64. Kornmüller, A.; Karcher, S.; Jekel, M. Adsorption of reactive dyes to granulated iron hydroxide and its oxidative regeneration. *Water Sci. Technol.* **2002**, *46*, 43–50. [[CrossRef](#)]
65. Nguyen Dang Giang, C.; Sebesvari, Z.; Renaud, F.; Rosendahl, I.; Hoang Minh, Q.; Amelung, W. Occurrence and Dissipation of the Antibiotics Sulfamethoxazole, Sulfadiazine, Trimethoprim, and Enrofloxacin in the Mekong Delta, Vietnam. *PLoS ONE* **2015**, *10*, e01318552015. [[CrossRef](#)]
66. Esteki, M.; Dashtaki, E.; Heyden, Y.V.; Simal-Gandara, J. Application of Rank Annihilation Factor Analysis for Antibacterial Drugs Determination by Means of pH Gradual Change-UV Spectral Data. *Antibiotics* **2020**, *9*, 383. [[CrossRef](#)]
67. Headley, J.V.; McMartin, D.W. A Review of the Occurrence and Fate of Naphthenic Acids in Aquatic Environments. *J. Environ. Sci. Health A* **2004**, *39*, 1989–2010. [[CrossRef](#)]
68. Psaltou, S.; Kaprara, E.; Triantafyllidis, K.; Mitrakas, M.; Zouboulis, A. Heterogeneous catalytic ozonation: The significant contribution of PZC value and wettability of the catalysts. *J. Environ. Chem. Eng.* **2021**, *9*, 106173. [[CrossRef](#)]
69. Wu, D.; Liu, Y.; He, H.; Zhang, Y. Magnetic pyrite cinder as an efficient heterogeneous ozonation catalyst and synergetic effect of deposited Ce. *Chemosphere* **2016**, *155*, 127–134. [[CrossRef](#)]
70. Zhang, F.; Wei, C.; Wu, K.; Zhou, H.; Hu, Y.; Preis, S. Mechanistic evaluation of ferrite AFe₂O₄ (A=Co, Ni, Cu, and Zn) catalytic performance in oxalic acid ozonation. *Appl. Catal. A Gen.* **2017**, *547*, 60–68. [[CrossRef](#)]
71. Morgan, J.J.; Stumm, W. Colloid-chemical properties of manganese dioxide. *J. Colloid Sci.* **1964**, *19*, 347–359. [[CrossRef](#)]
72. Rajput, S.; Pittman, C.U.; Mohan, D. Magnetic magnetite (Fe₃O₄) nanoparticle synthesis and applications for lead (Pb²⁺) and chromium (Cr⁶⁺) removal from water. *J. Colloid Interface Sci.* **2016**, *468*, 334–346. [[CrossRef](#)] [[PubMed](#)]
73. Farooq, M.; Ramli, A.; Subbarao, D. Physicochemical Properties of γ -Al₂O₃-MgO and γ -Al₂O₃-CeO₂ Composite Oxides. *J. Chem. Eng. Data* **2012**, *57*, 26–32. [[CrossRef](#)]
74. Salla, J.S.; Padoin, N.; Amorim, S.M.; Li Puma, G.; Moreira, R.F.M. Humic acids adsorption and decomposition on Mn₂O₃ and α -Al₂O₃ nanoparticles in aqueous suspensions in the presence of ozone. *J. Environ. Chem. Eng.* **2020**, *8*, 102780. [[CrossRef](#)]
75. Qi, F.; Xu, B.; Chen, Z.; Ma, J.; Sun, D.; Zhang, L. Influence of aluminum oxides surface properties on catalyzed ozonation of 2,4,6-trichloroanisole. *Sep. Purify. Technol.* **2009**, *66*, 405–410. [[CrossRef](#)]
76. Ikhtlaq, A.; Brown, D.R.; Kasprzyk-Hordern, B. Catalytic ozonation for the removal of organic contaminants in water on alumina. *Appl. Catal. B Environ.* **2015**, *165*, 408–418. [[CrossRef](#)]
77. Naeem, A.; Saddique, M.T.; Mustafa, S.; Kim, Y.; Dilara, B. Cation exchange removal of Pb from aqueous solution by sorption onto NiO. *J. Hazard. Mater.* **2009**, *168*, 364–368. [[CrossRef](#)] [[PubMed](#)]
78. Chen, H.; Wang, J. Catalytic ozonation for degradation of sulfamethazine using NiCo₂O₄ as catalyst. *Chemosphere* **2021**, *268*, 128840. [[CrossRef](#)]
79. Li, F.; Geng, D.; Cao, Q. Adsorption of As(V) on aluminum-, iron-, and manganese-(oxyhydr)oxides: Equilibrium and kinetics. *Desalin. Water Treat.* **2015**, *56*, 1829–1838. [[CrossRef](#)]
80. Pirovano, C.; Trasatti, S. The point of zero charge of Co₃O₄, Effect of the preparation procedure. *J. Electroanal. Chem. Interf. Electrochem.* **1984**, *180*, 171–184. [[CrossRef](#)]
81. Lu, J.; Wei, X.; Chang, Y.; Tian, S.; Xiong, Y. Role of Mg in mesoporous MgFe₂O₄ for efficient catalytic ozonation of Acid Orange II. *J. Chem. Technol. Biotechnol.* **2016**, *91*, 985–993. [[CrossRef](#)]
82. Sousa, V.S.; Teixeira, M.R. Aggregation kinetics and surface charge of CuO nanoparticles: The influence of pH, ionic strength and humic acids. *Environ. Chem.* **2013**, *10*, 313–322. [[CrossRef](#)]
83. Tengvall, P. 4.6 Protein Interactions with Biomaterials ☆. In *Comprehensive Biomaterials II*; Ducheyne, Ed.; Elsevier: Oxford, UK, 2017; pp. 70–84.
84. Parks, G.A.; Bruyn, L.D. The Zero Point of Charge of Oxides1. *J. Phys. Chem.* **1962**, *66*, 967–973. [[CrossRef](#)]
85. Kong, L.; Diao, Z.; Chang, X.; Xiong, Y.; Chen, D. Synthesis of recoverable and reusable granular MgO-SCCA-Zn hybrid ozonation catalyst for degradation of methylene blue. *J. Environ. Chem. Eng.* **2016**, *4*, 4385–4391. [[CrossRef](#)]
86. Faria, C.C.; Órfão, J.J.M.; Pereira, M.F.R. Activated carbon and ceria catalysts applied to the catalytic ozonation of dyes and textile effluents. *Appl. Catal. B Environ.* **2009**, *88*, 341–350. [[CrossRef](#)]
87. Chen, C.; Chen, Y.; Yoza, B.A.; Du, Y.; Wang, Y.; Li, Q.X.; Yi, L.; Guo, S.; Wang, Q. Comparison of Efficiencies and Mechanisms of Catalytic Ozonation of Recalcitrant Petroleum Refinery Wastewater by Ce, Mg, and Ce-Mg Oxides Loaded Al₂O₃. *Catalysts* **2017**, *7*, 72. [[CrossRef](#)]
88. Moussavi, G.; Mahmoudi, M. Degradation and biodegradability improvement of the reactive red 198 azo dye using catalytic ozonation with MgO nanocrystals. *Chem. Eng. J.* **2009**, *152*, 1–7. [[CrossRef](#)]
89. Oputu, O.; Chowdhury, M.; Nyamayaro, K.; Fatoki, O.; Fester, V. Catalytic activities of ultra-small β -FeOOH nanorods in ozonation of 4-chlorophenol. *J. Environ. Sci.* **2015**, *35*, 83–90. [[CrossRef](#)]

90. Ziyilan-Yavaş, A.; Ince, N.H. Catalytic ozonation of paracetamol using commercial and Pt-supported nanocomposites of Al₂O₃, The impact of ultrasound. *Ultrason. Sonochem.* **2018**, *40*, 175–182. [[CrossRef](#)]
91. Moussavi, G.; Khavanin, A.; Alizadeh, R. The integration of ozonation catalyzed with MgO nanocrystals and the biodegradation for the removal of phenol from saline wastewater. *Appl. Catal. B Environ.* **2010**, *97*, 160–167. [[CrossRef](#)]
92. Aghaeinejad-Meybodi, A.; Ebadi, A.; Shafiei, S.; Khataee, A.; Kiadehi, A.D. Degradation of Fluoxetine using catalytic ozonation in aqueous media in the presence of nano- γ -alumina catalyst: Experimental, modeling and optimization study. *Sep. Purify. Technol.* **2019**, *211*, 551–563. [[CrossRef](#)]
93. Aguilar, C.M.; Vazquez-Arenas, J.; Castillo-Araiza, O.O.; Rodríguez, J.L.; Chairez, I.; Salinas, E.; Poznyak, T. Improving ozonation to remove carbamazepine through ozone-assisted catalysis using different NiO concentrations. *Environ. Sci. Pollut. Res.* **2020**, *27*, 22184–22194. [[CrossRef](#)] [[PubMed](#)]
94. Gonçalves, A.G.; Órfão, J.J.M.; Pereira, M.F.R. Ceria dispersed on carbon materials for the catalytic ozonation of sulfamethoxazole. *J. Environ. Chem. Eng.* **2013**, *1*, 260–269. [[CrossRef](#)]
95. Vittenet, J.; Aboussaoud, W.; Mendret, J.; Pic, J.-S.; Debellefontaine, H.; Lesage, N.; Faucher, K.; Manero, M.-H.; Thibault-Starzyk, F.; Leclerc, H.; et al. Catalytic ozonation with γ -Al₂O₃ to enhance the degradation of refractory organics in water. *Appl. Catal. A Gen.* **2015**, *504*, 519–532. [[CrossRef](#)]
96. He, Y.; Zhang, H.; Li, J.J.; Zhang, Y.; Lai, B.; Pan, Z. Treatment of Landfill Leachate Reverse Osmosis Concentrate from by Catalytic Ozonation with γ -Al₂O₃. *Environ. Sci.* **2018**, *35*, 501–511. [[CrossRef](#)]
97. Polat, D.; Balci, İ.; Özbelge, T.A. Catalytic ozonation of an industrial textile wastewater in a heterogeneous continuous reactor. *J. Environ. Chem. Eng.* **2015**, *3*, 1860–1871. [[CrossRef](#)]
98. Nawaz, F.; Xie, Y.; Cao, H.; Xiao, J.; Wang, Y.; Zhang, X.; Li, M.; Duan, F. Catalytic ozonation of 4-nitrophenol over an mesoporous α -MnO₂ with resistance to leaching. *Catal. Today* **2015**, *258*, 595–601. [[CrossRef](#)]
99. Nemati Sani, O.; Navaei fezabady, A.A.; Yazdani, M.; Taghavi, M. Catalytic ozonation of ciprofloxacin using γ -Al₂O₃ nanoparticles in synthetic and real wastewaters. *J. Water Process. Eng.* **2019**, *32*, 100894. [[CrossRef](#)]
100. Wang, S.; Zhou, L.; Zheng, M.; Han, J.; Liu, R.; Yun, J. Catalytic Ozonation over Ca₂Fe₂O₅ for the Degradation of Quinoline in an Aqueous Solution. *Ind. Eng. Chem. Res.* **2022**, *61*, 6343–6353. [[CrossRef](#)]
101. He, C.; Chen, Y.; Guo, L.; Yin, R.; Qiu, T. Catalytic ozonation of NH₄⁺-N in wastewater over composite metal oxide catalyst. *J. Rare Earths* **2022**, *40*, 73–84. [[CrossRef](#)]
102. Al jibouri, A.K.H.; Wu, J.; Upreti, S.R. Heterogeneous catalytic ozonation of naphthenic acids in water. *Can. J. Chem. Eng.* **2019**, *97*, 67–73. [[CrossRef](#)]
103. Li, G.; Lu, Y.; Lu, C.; Zhu, M.; Zhai, C.; Du, Y.; Yang, P. Efficient catalytic ozonation of bisphenol-A over reduced graphene oxide modified sea urchin-like α -MnO₂ architectures. *J. Hazard. Mater.* **2015**, *294*, 201–208. [[CrossRef](#)] [[PubMed](#)]
104. Yin, R.; Guo, W.; Zhou, X.; Zheng, H.; Du, J.; Wu, Q.; Chang, J.; Ren, N. Enhanced sulfamethoxazole ozonation by noble metal-free catalysis based on magnetic Fe₃O₄ nanoparticles: Catalytic performance and degradation mechanism. *RSC Adv.* **2016**, *6*, 19265–19270. [[CrossRef](#)]
105. Luo, K.; Zhao, S.-X.; Wang, Y.-F.; Zhao, S.-J.; Zhang, X.-H. Synthesis of petal-like δ -MnO₂ and its catalytic ozonation performance. *New J. Chem.* **2018**, *42*, 6770–6777. [[CrossRef](#)]
106. Bai, Z.; Yang, Q.; Wang, J. Catalytic ozonation of sulfamethazine using Ce_{0.1}Fe_{0.9}OOH as catalyst: Mineralization and catalytic mechanisms. *Chem. Eng. J.* **2016**, *300*, 169–176. [[CrossRef](#)]
107. Beltrán, F.J.; Pocostales, P.; Álvarez, M.; López-Piñeiro, F. Catalysts to improve the abatement of sulfamethoxazole and the resulting organic carbon in water during ozonation. *Appl. Catal. B Environ.* **2009**, *92*, 262–270. [[CrossRef](#)]
108. Chen, J.; Tu, Y.; Shao, G.; Zhang, F.; Zhou, Z.; Tian, S.; Ren, Z. Catalytic ozonation performance of calcium-loaded catalyst (Ca-C/Al₂O₃) for effective treatment of high salt organic wastewater. *Sep. Purify. Technol.* **2022**, *301*, 121937. [[CrossRef](#)]
109. Liu, H.; Gao, Y.; Wang, J.; Pan, J.; Gao, B.; Yue, Q. Catalytic ozonation performance and mechanism of Mn-CeOx@ γ -Al₂O₃/O₃ in the treatment of sulfate-containing hypersaline antibiotic wastewater. *Sci. Total Environ.* **2022**, *807*, 150867. [[CrossRef](#)]
110. Jeirani, Z.; Soltan, J. Improved formulation of Fe-MCM-41 for catalytic ozonation of aqueous oxalic acid. *Chem. Eng. J.* **2017**, *307*, 756–765. [[CrossRef](#)]
111. Guo, H.; Li, X.; Li, G.; Liu, Y.; Rao, P. Preparation of SnO_x-MnO_x@Al₂O₃ for Catalytic Ozonation of Phenol in Hypersaline Wastewater. *Ozone Sci. Eng.* **2022**, 1–14. [[CrossRef](#)]
112. Afzal, S.; Quan, X.; Chen, S.; Wang, J.; Muhammad, D. Synthesis of manganese incorporated hierarchical mesoporous silica nanosphere with fibrous morphology by facile one-pot approach for efficient catalytic ozonation. *J. Hazard. Mater.* **2016**, *318*, 308–318. [[CrossRef](#)] [[PubMed](#)]
113. Bing, J.; Hu, C.; Zhang, L. Enhanced mineralization of pharmaceuticals by surface oxidation over mesoporous γ -Ti-Al₂O₃ suspension with ozone. *Appl. Catal. B Environ.* **2017**, *202*, 118–126. [[CrossRef](#)]
114. Chen, W.; Li, X.; Pan, Z.; Ma, S.; Li, L. Effective mineralization of Diclofenac by catalytic ozonation using Fe-MCM-41 catalyst. *Chem. Eng. J.* **2016**, *304*, 594–601. [[CrossRef](#)]
115. Li, H.; Huang, Y.; Cui, S. Removal of alachlor from water by catalyzed ozonation on Cu/Al₂O₃honeycomb. *Chem. Cent. J.* **2013**, *7*, 143. [[CrossRef](#)]
116. Feng, C.; Zhao, J.; Qin, G.; Diao, P. Construction of the Fe³⁺-O-Mn^{3+/2+} hybrid bonds on the surface of porous silica as active centers for efficient heterogeneous catalytic ozonation. *J. Solid State Chem.* **2021**, *300*, 122266. [[CrossRef](#)]

117. Chen, W.; Li, X.; Pan, Z.; Ma, S.; Li, L. Synthesis of MnO_x/SBA-15 for Norfloxacin degradation by catalytic ozonation. *Sep. Purify. Technol.* **2017**, *173*, 99–104. [[CrossRef](#)]
118. Liu, X.; Wang, S.; Yang, H.; Liu, Z.; Wang, Y.; Meng, F.; Ma, J.; Izosimova, O.S. Characterization of a Doped MnO₂Al₂O₃ Catalyst and its Application Inmicrobubble Ozonation for Quinoline Degradation. *Ozone Sci. Eng.* **2021**, *43*, 173–184. [[CrossRef](#)]
119. Gao, G.; Shen, J.; Chu, W.; Chen, Z.; Yuan, L. Mechanism of enhanced diclofenac mineralization by catalytic ozonation over iron silicate-loaded pumice. *Sep. Purify. Technol.* **2017**, *173*, 55–62. [[CrossRef](#)]
120. Liu, Y.; Wang, S.; Gong, W.; Chen, Z.; Liu, H.; Bu, Y.; Zhang, Y. Heterogeneous catalytic ozonation of p-chloronitrobenzene (pCNB) in water with iron silicate doped hydroxylation iron as catalyst. *Catal. Common.* **2017**, *89*, 81–85. [[CrossRef](#)]
121. Mohammadi, V.; Tabatabaee, M.; Fadaei, A.; Mirhoseini, S.A. Study of Nickel Nanoparticles in Highly Porous Nickel Metal–Organic Framework for Efficient Heterogeneous Catalytic Ozonation of Linear Alkyl Benzene Sulfonate in Water. *Ozone Sci. Eng.* **2021**, *43*, 239–253. [[CrossRef](#)]
122. Yang, W.; Wu, T. Investigation of Matrix Effects in Laboratory Studies of Catalytic Ozonation Processes. *Ind. Eng. Chem. Res.* **2019**, *58*, 3468–3477. [[CrossRef](#)]
123. Xing, S.; Lu, X.; Liu, J.; Zhu, L.; Ma, Z.; Wu, Y. Catalytic ozonation of sulfosalicylic acid over manganese oxide supported on mesoporous ceria. *Chemosphere* **2016**, *144*, 7–12. [[CrossRef](#)]
124. Chen, H.; Wang, J. Catalytic ozonation of sulfamethoxazole over Fe₃O₄/Co₃O₄ composites. *Chemosphere* **2019**, *234*, 14–24. [[Cross-Ref](#)]
125. Martins, R.C.; Cardoso, M.; Dantas, R.F.; Sans, C.; Esplugas, S.; Quinta-Ferreira, R.M. Catalytic studies for the abatement of emerging contaminants by ozonation. *J. Chem. Technol. Biotechnol.* **2015**, *90*, 1611–1618. [[CrossRef](#)]
126. Yan, J.; Lai, L.; Ji, F.; Zhang, Y.; Li, Y.; Lai, B. Catalytic Ozonation of Sulfamethoxazole in the Presence of CuO/Al₂O₃-EPC: Optimization, Degradation Pathways, and Toxicity Evaluation. *Environ. Eng. Sci.* **2019**, *36*, 912–921. [[CrossRef](#)]
127. Shahidi, D.; Moheb, A.; Abbas, R.; Larouk, S.; Roy, R.; Azzouz, A. Total mineralization of sulfamethoxazole and aromatic pollutants through Fe²⁺-montmorillonite catalyzed ozonation. *J. Hazard. Mater.* **2015**, *298*, 338–350. [[CrossRef](#)] [[PubMed](#)]
128. Wu, J.; Gao, H.; Yao, S.; Chen, L.; Gao, Y.; Zhang, H. Degradation of Crystal Violet by catalytic ozonation using Fe/activated carbon catalyst. *Sep. Purify. Technol.* **2015**, *147*, 179–185. [[CrossRef](#)]
129. Gonçalves, A.G.; Órfão, J.J.M.; Pereira, M.F.R. Catalytic ozonation of sulphamethoxazole in the presence of carbon materials: Catalytic performance and reaction pathways. *J. Hazard. Mater.* **2012**, *239*, 167–174. [[CrossRef](#)]
130. Akhtar, J.; Amin, N.S.; Aris, A. Combined adsorption and catalytic ozonation for removal of sulfamethoxazole using Fe₂O₃/CeO₂ loaded activated carbon. *Chem. Eng. J.* **2011**, *170*, 136–144. [[CrossRef](#)]
131. Gonçalves, A.G.; Órfão, J.J.M.; Pereira, M.F.R. Ozonation of sulfamethoxazole promoted by MWCNT. *Catal. Common.* **2013**, *35*, 82–87. [[CrossRef](#)]
132. Huang, Y.; Sun, Y.; Xu, Z.; Luo, M.; Zhu, C.; Li, L. Removal of aqueous oxalic acid by heterogeneous catalytic ozonation with MnO_x/sewage sludge-derived activated carbon as catalysts. *Sci. Total Environ.* **2017**, *575*, 50–57. [[CrossRef](#)] [[PubMed](#)]
133. Zhang, J.; Guo, Q.; Wu, W.; Shao, S.; Li, Z.; Liu, Y.; Jiao, W. Preparation of Fe-MnO_x/AC by high gravity method for heterogeneous catalytic ozonation of phenolic wastewater. *Chem. Eng. Sci.* **2022**, *255*, 117667. [[CrossRef](#)]
134. Shahamat, Y.D.; Farzadkia, M.; Nasseri, S.; Mahvi, A.H.; Gholami, M.; Esrafil, A. Magnetic heterogeneous catalytic ozonation: A new removal method for phenol in industrial wastewater. *J. Environ. Health Sci. Eng.* **2014**, *12*, 50. [[CrossRef](#)] [[PubMed](#)]
135. Wang, Y.; Xie, Y.; Sun, H.; Xiao, J.; Cao, H.; Wang, S. Efficient Catalytic Ozonation over Reduced Graphene Oxide for p-Hydroxybenzoic Acid (PHBA) Destruction: Active Site and Mechanism. *ACS Appl. Mater. Interfaces* **2016**, *8*, 9710–9720. [[Cross-Ref](#)]
136. Jothinathan, L.; Hu, J. Kinetic evaluation of graphene oxide based heterogenous catalytic ozonation for the removal of ibuprofen. *Water Res.* **2018**, *134*, 63–73. [[CrossRef](#)]
137. Yin, R.; Guo, W.; Du, J.; Zhou, X.; Zheng, H.; Wu, Q.; Chang, J.; Ren, N. Heteroatoms doped graphene for catalytic ozonation of sulfamethoxazole by metal-free catalysis: Performances and mechanisms. *Chem. Eng. J.* **2017**, *317*, 632–639. [[CrossRef](#)]
138. Kosmulski, M. pH-dependent surface charging and points of zero charge. IV. Update and new approach. *J. Colloid Interface Sci.* **2009**, *337*, 439–448. [[CrossRef](#)]
139. Huang, Y.; Cui, C.; Zhang, D.; Li, L.; Pan, D. Heterogeneous catalytic ozonation of dibutyl phthalate in aqueous solution in the presence of iron-loaded activated carbon. *Chemosphere* **2015**, *119*, 295–301. [[CrossRef](#)]
140. Karimi, M.; Sadeghi, S.; Mohebbali, H.; Azarkhosh, Z.; Safarifard, V.; Mahjoub, A.; Heydari, A. Fluorinated solvent-assisted photocatalytic aerobic oxidative amidation of alcohols via visible-light-mediated HKUST-1/Cs-POMoW catalysis. *New J. Chem.* **2021**, *45*, 14024–14035. [[CrossRef](#)]
141. Karimi, M.; Mohebbali, H.; Sadeghi, S.; Safarifard, V.; Mahjoub, A.; Heydari, A. Additive-free aerobic C-H oxidation through a defect-engineered Ce-MOF catalytic system. *Microporous Mesoporous Mater.* **2021**, *322*, 111054. [[CrossRef](#)]
142. Rozveh, Z.S.; Kazemi, S.; Karimi, M.; Ali, G.A.M.; Safarifard, V. Effect of functionalization of metal-organic frameworks on anion sensing. *Polyhedron* **2020**, *183*, 114514. [[CrossRef](#)]
143. Liao, X.; Wang, F.; Wang, Y.; Cai, Y.; Liu, H.; Wang, X.; Zhu, Y.; Chen, L.; Yao, Y.; Hao, Q. Constructing Fe-based bi-MOFs for photo-catalytic ozonation of organic pollutants in Fischer-Tropsch waste water. *Appl. Surf. Sci.* **2020**, *509*, 145378. [[CrossRef](#)]
144. Chávez, A.M.; Rey, A.; López, J.; Álvarez, M.; Beltrán, F.J. Critical aspects of the stability and catalytic activity of MIL-100(Fe) in different advanced oxidation processes. *Sep. Purify. Technol.* **2021**, *255*, 117660. [[CrossRef](#)]

145. Ye, G.; Luo, P.; Zhao, Y.; Qiu, G.; Hu, Y.; Preis, S.; Wei, C. Three-dimensional Co/Ni bimetallic organic frameworks for high-efficient catalytic ozonation of atrazine: Mechanism, effect parameters, and degradation pathways analysis. *Chemosphere* **2020**, *253*, 126767. [[CrossRef](#)] [[PubMed](#)]
146. Zheng, H.; Hou, Y.; Li, S.; Ma, J.; Nan, J.; Li, T. Recent advances in the application of metal organic frameworks using in advanced oxidation progresses for pollutants degradation. *Chin. Chem. Lett.* **2022**, *33*, 5013–5022. [[CrossRef](#)]
147. Chen, H.; Wang, J. MOF-derived Co₃O₄-C@FeOOH as an efficient catalyst for catalytic ozonation of norfloxacin. *J. Hazard. Mater.* **2021**, *403*, 123697. [[CrossRef](#)]
148. Hu, Q.; Zhang, M.; Xu, L.; Wang, S.; Yang, T.; Wu, M.; Lu, W.; Li, Y.; Yu, D. Unraveling timescale-dependent Fe-MOFs crystal evolution for catalytic ozonation reactivity modulation. *J. Hazard. Mater.* **2022**, *431*, 128575. [[CrossRef](#)]
149. Hu, Q.; Xu, L.; Fu, K.; Zhu, F.; Yang, T.; Yang, T.; Luo, J.; Wu, M.; Yu, D. Ultrastable MOF-based foams for versatile applications. *Nano Res.* **2022**, *15*, 2961–2970. [[CrossRef](#)]
150. Pang, Z.; Luo, P.; Wei, C.; Qin, Z.; Wei, T.; Hu, Y.; Wu, H.; Wei, C. In-situ growth of Co/Ni bimetallic organic frameworks on carbon spheres with catalytic ozonation performance for removal of bio-treated coking wastewater. *Chemosphere* **2022**, *291*, 132874. [[CrossRef](#)]
151. Yu, D.; Wu, M.; Hu, Q.; Wang, L.; Lv, C.; Zhang, L. Iron-based metal-organic frameworks as novel platforms for catalytic ozonation of organic pollutant: Efficiency and mechanism. *J. Hazard. Mater.* **2019**, *367*, 456–464. [[CrossRef](#)]

Disclaimer/Publisher's Note: The statements, opinions and data contained in all publications are solely those of the individual author(s) and contributor(s) and not of MDPI and/or the editor(s). MDPI and/or the editor(s) disclaim responsibility for any injury to people or property resulting from any ideas, methods, instructions or products referred to in the content.